UNIVERSITY OF CALIFORNIA SAN DIEGO

Toward the Development of Allosteric Inhibitors of IKK2

A Thesis submitted in partial satisfaction of the requirements
for the degree Master of Science

in

Chemistry

by

Sonjiala Jackson Hotchkiss

Committee in charge:

Professor Gourisankar Ghosh, Chair
Professor Elizabeth Komives
Professor Dionicio Siegel

2018

The Thesis of Sonjiala Jackson Hotchkiss is approved, and it is acceptable in quality and form for publication on microfilm and electronically:

_____

_____

_____

Chair

University of California San Diego

2018

DEDICATION

This Thesis is dedicated to my spouse Lee Hotchkiss and to Charlie, the schnoodle and the COO our little pack.

TABLE OF CONTENTS

Signature Page iii

Dedication iv

Table of Contents v

List of Abbreviations viii

List of Figures x

List of Tables xii

Acknowledgement xiii

Abstract of the Thesis xv

I. Introduction 1

A. NF-κB Discovery and Function 2

B. IKK: Activator of NF-κB 5

C. Activation Pathways of NF-κB 7

D. NF-κB and Disease 9

E. Inhibitors of IKK2 10

G. Focus of Study 11

II. Materials and Methods 12

A. Baculovirus Expression 13

1.Sf9 Cell Culturing 13

2. Preparation of Plasmid/Bacmid 13

3. Viral Amplification 13

4. Large-Scale Protein Expression 14

5. Lysis of Sf9 Cells 14
B. Protein Purification Protocols 15
1. Batch Binding Using Nickel Beads 15
2. Size-Exclusion Column Chromatography 15
C. *In vivo* Assays 15
1. IKK2 Inhibitor Assays 15
D. *In vitro* Assays 16
1. IKK2 Kinase Assay 16
2. IKK2-Inhibitor Kinase Assays 16
E. Western Blot 16
1. Antibodies 16
2. Procedure 16
F. Hydrogen-Deuterium Exchange Mass Spectrometry 17
G. Crystallography 18
F. Mass Spectrometry 18
III. Results 19
A. IKK2 11-669 EE Expression and Purification 20
B. IKK2 11-669 EE is more active *in vitro* than FL IKK2 EE 23
C. #65.5 inhibits IKK activation *in vivo* 23
D. #65.5 does not inhibit catalytic activity of active IKK2 24
E. Hydrogen-Deuterium Exchange Mass Spectrometry Data 25
1. Dynamic Segments of IKK2 11-669 EE map within the loop and linker region 26

2. Protection of only two peptides is different with # 65.5.3 bound 29

3. TPCA1 and ATP protect distinct but overlapping segments 32

4. Both #65.5 and #65.5.3 covalently cross-linked to IKK2 11-669 EE 34

IV. Discussion 37

References 43

LIST OF ABBREVIATIONS

ARD	ankyrin repeats domain
BAFF	B-cell activating factor
BME	β-mercaptoethanol
BSA	bovine serum albumin
CD40	cluster of differentiation 40
DD	dimerization domain
DeD	death domain
DMEM	Dulbecco's Modified Eagle Medium
DTT	dithiothreitol
ECL	enhanced chemiluminescence
FBS	fetal bovine serum
FL	full-length
GRR	glycine rich repeat
IκB	inhibitor of NF-κB
IKK	inhibitor of NF-κB kinase
kDa	kilodalton
LT-beta	Lymphotoxin-beta
MBD	magnesium binding loop

MW	molecular weight
NEMO	NF-κB essential modulator
NF-κB	nuclear factor kappa B
NIK	NF-κB inducing kinase
NLS	nuclear localization sequence
NTD	N-terminal domain
PAGE	polyacrylamide gel electrophoresis
PEST	sequence rich in Pro, Glu, Ser and Thr
PIC	protease inhibitor cocktail
PMSF	phenylmethylsulfonyl fluoride
PSG	penicillin-atreptomycin-glutamine
RHR	Rel homology region
Sf9	*Spodoptera frugiperda* 9
SDS	sodium dodecyl sulfate
SP	serine-proline
TAD	transcriptional activation domain

LIST OF FIGURES

Figure 1.1. Schematic representation of the members of the NF-κB family 4

Figure 1.2. Schematic representation of the members of the IκB family 5

Figure 1.3. Schematic representation of IKK proteins 6

Figure 1.4. Schematic representation of IKK2 along with structure 6

Figure 1.5. Two major NF-κB activation pathways 8

Figure 3.1. Purification of truncated IKK2 11-669 EE.....21

Figure 3.2. Nickel-purified and TEV and ATP-treated IKK2 11-669 EE was loaded onto a superose 6 size exclusion column 22

Figure 3.3. In vitro kinase assay of IKK2 11-669 EE and IKK2 FL EE with IκBα substrate 23

Figure 3.4. *In vivo* assays of inhibitor efficacy by looking at IκBα degradation and inhibitor structure 24

Figure 3.5. *In vitro* kinase assay showing effect of inhibitor on IKK2 EE kinase activity 25

Figure 3.6. Color-coded representation of IKK2 11-669 EE protein dynamics 28

Figure 3.7. HDX residues 115-125 and 117-125 and Legend for HDX 29

Figure 3.8. Residues 15-40, 41-61, 61-75, 151-168, 161-168.....30

Figure 3.9. Residues 213-242, 243-265, 243-255.....31

Figure 3.10. HDX residues 360-383 and 360-386.....31

Figure 3.11. HDX residues 466-475 and 466-485, 280-300, 571-590, and 632-646.....32

Figure 3.12. HDX residues 492-503 and 494-503, 548-563.....32

Figure 3.13. HDX residues 30-40, 76-94, 76-95, 76-96 34

Figure 3.14. HDX residues 15-29, 96-110, and 98-110.....34

Figure 3.15. The binding pocket for inhibitor #65.5.3.....36

Figure 3.16. Our model of how inhibitor #65.5.3 works.....42

LIST OF TABLES

Table 1.1. The IC_{50} values for the synthesized inhibitors 11

Table 3.1. MS-MS data showing mass changes on cysteines 114 and 115 with inhibitor bound to IKK2 11-669 EE 35

ACKNOWLEDGEMENT

I would like to acknowledge the people who played crucial roles in supporting me on my path to being a research scientist at UCSD. Foremost, I thank my principle investigator, Professor Gourisankar Ghosh. Even before joining his lab I was encouraged and inspired by his commitment to professionalism and his passion for learning and for research. I can think of no better way to honor his investment of time and belief in my development than by dedicating myself to my research and always being mindful of the precious opportunity to do so, particularly at an institution as distinguished as UCSD.

I would also like to thank Professor Elizabeth Komives, my champion, who has been endlessly generous with her time and her assistance. My continued studies may not have been possible without her assistance. I would also like to thank Professor Professor Dionicio Siegel for agreeing to be a member of my committee and for being our collaborator by synthesizing the inhibitor compounds used in this research.

My colleagues in the lab have been crucial to my development. All have shared both knowledge and kindness in double measure and without hesitation. I will be forever grateful to Dr. Maria Mulero-Roig especially and also Dr. Tapan Biswas, Boqing Gu, Shandy Shahabi, Myung Ko, Dr. Kaushik Saha, Kyle Shumate, Samantha Cohen, Dr. Yidan Li, Dr. Anup Mazumder, Dr. Vivien Wang, Qian Du, Mike Fernandez, Jehanne Aghzadi, Daniel Kim, and Sarah Fulop. I give special acknowledgment to Myung Ko for her assistance in performing kinase assays with truncated and full-length IKK2 and also again to Professor Ghosh for providing experimental data on kinase function of IKK2 with inhibitors SC514 and #65.5.3.

Before I continued graduate study at UCSD, I received years of support and encouragement from Dr. Edward Alexander my PI as a member of the Bridges to the Baccalaureate Program. He did so much to make the transition from being a history major to being a UCSD graduate student

in chemistry possible. I will always aspire to approach his example of being a generous and relentless mentor. I would also like to especially thank fellow Bridges researcher Samantha Barrera and all my other Bridges colleagues.

I give a special thank you to those from the community who never doubted that I had the ability to fulfill my audacious ambitions especially Dr. Daniel O'Roarty and Daniel Valdivia. I feel great sorrow that Daniel Valdivia has passed on without seeing me achieve this goal, but I am grateful for his influence on my thinking and for his example of being ever compassionate toward and helpful to those in need. In addition, I thank friends and family their support.

Finally, I would like to acknowledge my spouse Lee Hotchkiss, and our beloved dog Charlie for their love and companionship. The journey to this point was a long one over many years, but all along the way there were three little sets of foot prints two of two and one of four.

ABSTRACT OF THE THESIS

Toward the Development of Allosteric Inhibitors of IKK2

by

Sonjiala Jackson Hotchkiss

Master of Science in Chemistry

University of California San Diego, 2018

Professor Gourisankar Ghosh, Chair

IκB kinase (IKK) is the essential kinase in the activation pathway of NF-κB, a family of transcription factors active in both innate and adaptive immunity. IKK has two catalytic subunits, IKK1 and IKK2, and one scaffolding subunit NEMO. As aberrant activation of NF-κB is a factor in many diseases including cancer and inflammatory disorders, research has been directed toward developing inhibitors to its activation. Most developed inhibitors target IKK2 and work as ATP competitors. However, ATP competitive inhibitors are often too nonspecific and have too many adverse side effects to be developed as effective drug treatments. I tested and characterized the function of small molecule allosteric inhibitors identified by our lab named #65.5, #65.5.2, and

#65.5.3. Allosteric inhibitors of IKK2 are expected to result in greater specificity with fewer adverse side effects. I used cell-based assays, kinase experiments, HDXMS, and MS-MS to confirm that our inhibitors prevented NF-κB activation, worked as allosteric inhibitors, and bound to the pocket predicted by virtual screening. Based on analysis of the collected data, we developed a model for how our inhibitors work to prevent IKK2 activation.

I. Introduction

A. NF-κB Discovery and Function

While the Baltimore lab was studying the transcription of the κ light chain gene in B cells, they discovered an enhancer of the gene that was necessary to activate the expression of the κ gene. This enhancer was found exclusively in the κ light chain gene and not the λ heavy chain. Moreover, this enhancer DNA of sequence GGGACTTTCC specifically bound a protein factor (Baltimore, 2009; Sen and Baltimore, 1986). It became evident that interaction between the DNA and the new protein factor was essential for the κ gene transcription. Since the factor was found in the nucleus of B cells which activated the expression of the κ gene, they named the factor as Nuclear Factor of kappa in B cells (NF-κB).

Subsequent work in many different laboratories including the Baltimore laboratory determined that NF-κB is ubiquitously expressed in many cells and not just in B cells (Baeuerle and Baltimore, 1996; Baeuerle and Henkel, 1994; Baldwin, 1996; Ghosh et al., 1998). They found that unlike in mature B cells, where NF-κB is constitutively nuclear, in other cells NF-κB dimers dormant in the cytosol. That NF-κB exists in a dormant state was discovered by asking why cells known to have a rearranged κ light chains neither expressed these chains nor had detectable levels of the newly discovered enhancer protein (Baltimore, 2009). Lipopolysaccharide (LPS) was known to stimulate expression of κ light chain. This research question lead to the discovery that LPS could also lead to NF-κB activation and translocation from the cytoplasm to the nucleus (Baltimore, 2009).

NF-κB binds to a variety of κB DNA of the general form 5'-GGGRNWYYCC-3' (N, any base; R, purine; W, adenine or thymine; Y, pyrimidine) (Huxford, 2009; Chen,1998). As a nuclear transcription factor NF-κB is known to be involved in not only the activation of gene expression but also in the repression of a number of genes. These NF-κB effector genes have many functions. Most importantly they are involved in innate and adaptive immunity. Additionally, genes that

regulate apoptosis and genes that support cell survival and proliferation are also regulated by NF-κB (Baeuerle and Baltimore, 1996; Baeuerle and Henkel, 1994; Baldwin, 1996; Ghosh et al., 1998). This discovery that NF-κB could lay dormant in the cytoplasm of cells was an important step in uncovering its ubiquitous presence. The early experiments involved LPS stimulation, however, NF-κB can be activated by a number of stimuli including a variety of pro-inflammatory cytokines, viral factors, bacterial factors, radiation, and environmental stressors.

The first discovered form of NF-κB was the heterodimer purified in Baltimore's lab by Ranjan Sen. It was composed of a 50 kDa subunit, p50, and a 65 kDa subunit, p65 also known as RelA (Sen and Baltimore, 1986). The RelA/p50 heterodimer is the most abundant form of NF-κB. The complete family of NF-κB transcription factors has five members that combine to form up to 15 hetero- and homodimers: p65/RelA, p50, p52, c-Rel, and RelB. All five family members of NF-κB share an N-terminal region of sequence homology known as a rel homology region (RHR). This region consists of about 300 amino acids. It contains the DNA-binding domain and the dimerization domain joined by a short linker. A flexible segment at the C-terminus of the dimerization domain contains the nuclear localization signal (NLS). The rel members of the family, RelA/p65, c-Rel, and RelB contain a transactivation domain (TAD) not shared by the other two members (Hoffmann et al., 2006). This TAD distinguishes these members as activators of transcription. Both p50 and p52 result after cleavage of C-terminal auto-inhibitory regions for p105 and p100 respectively (Bours et al., 1990; Ghosh and Baltimore, 1990; Kieran et al., 1990). These two members of the family lack a TAD but share a glycine rich region at their C-terminal ends (Figure 1.1).

In its dormant state, NF-κB is held by a family of inhibitors known as IκBs. In the case of the RelA/p50 heterodimer, the dominant inhibitor is IκBα. Other known IκBs are IκBβ and IκBε

(Oeckinghaus and Ghosh, 2009). There are two major pathways of NF-κB activation, the canonical pathway and the non-canonical pathway (discussed below). Generally speaking, an extra-cellular signal stimulates an intracellular cascade that leads to the degradation of inhibitors of NF-κB, thus exposing its nuclear localization signal and freeing it to translocate to the nucleus to either enhance or repress transcription.

Central to NF-κB activation are the members of the hetero-trimer IκB Kinase (IKK). IKK consists of two catalytic subunits, IKK1 and IKK2, and one scaffolding subunit, NF-κB essential modulator (NEMO). Improperly regulated NF-κB activation is a factor in a host of diseases, most notably inflammatory disorders and cancers. Improper regulation of NF-κB is most associated with aberrant IKK2 activity. Thus many therapeutic interventions targeting NF-κB activation focus on the development of small molecule inhibitors of IKK2.

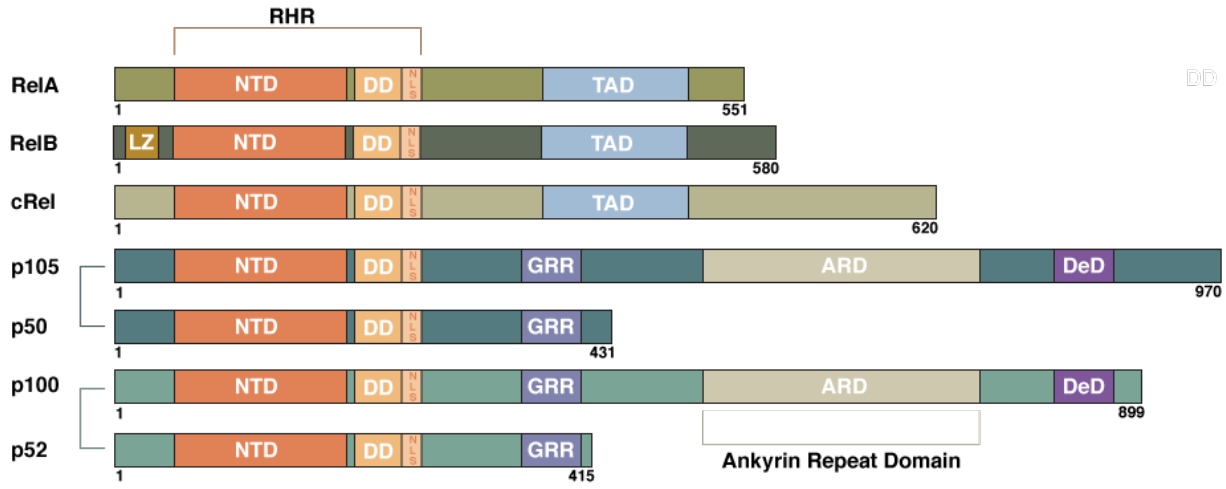

Figure 1.1. Schematic representation of the members of the NF-κB family.
The proteins in the NF-κB family share a Rel homology region. The RHR consists of the N-terminal domain (NTD) and a dimerization domain (DD). The DD contains the nuclear localization signal (NLS). RelA, RelB and cRel all contain a transactivation domain (TAD) that is important for activating transcription. In addition RelB has an n-terminal leucine zipper. The precursors to p50 and p52, p105 and p100 respectively, contain ankyrin repeats and death domains (DeD). The precursors along with p50 and p52 contain glycine rich regions (GRR).

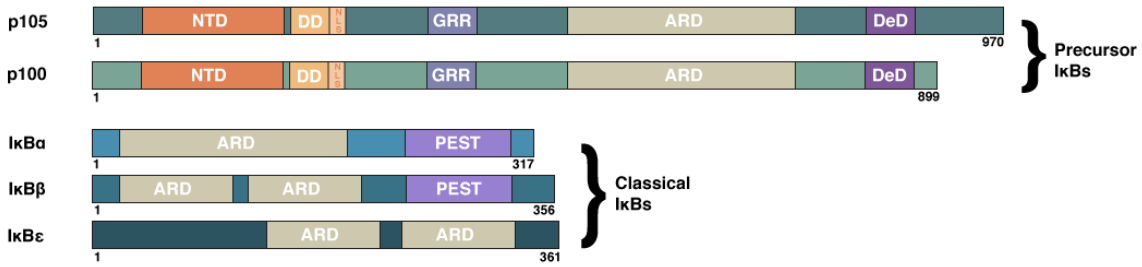

Figure 1.2. Schematic representation of the members of the IκB family.
Precursor and classical IκBs have ankyrin repeat domains (ARDs). Classical IκBs have a PEST region.

B. IKK: Activator of NF-κB

IKK was first identified as an IκBα kinase (Chen, 1996). It was later purified as a 700-900 kDa complex. IKK is currently described as consisting of three subunits. The two catalytic subunits, IKK1 and IKK2, contain a kinase domain and share 50% identity. The third subunit, NEMO, is a scaffolding domain that works to organize the catalytic subunits (Delhase et al., 1999). IKK1 and IKK2 are 85 and 87 kDa respectively, while NEMO is a 48 kDa protein. The exact composition of the IKK complex detailing the number(s) of each subunit present remains unknown.

Like all other protein kinases IKK1 and IKK2 contain 'activation loops' within their kinase domains. Phosphorylation of two activation loop serines mark IKK activation. These phosphorylations thus are part of the signaling cascade that begins at the cell surface and ends at generation of transcriptionally active NF-κB. The activation loop serines for IKK2 are at residues 177 and 181, while for IKK1 they are serine residues 176 and 180 (Delhase et al., 1999). The catalytic subunits can undergo autophosphorylation, but upstream kinases may also be involved in phosphorylating these kinases depending on the type of extracellular stimuli. Mutation of the activation loop serines in IKK2 to glutamic acid give the constitutively active conformation. Constitutively active, truncated IKK2 has been used in the experiments discussed in this thesis, IKK2 (11-669 EE).

IKK1 and IKK2 have a similar protein structure. They contain an N-terminal kinase domain (KD), a ubiquitin-like domain (ULD), a scaffolding dimerization domain (SDD), a serine rich region (S), and a c-terminal NEMO binding domain (N) (Figure 1.3). The NEMO binding domain binds stably with NEMO. NEMO contains two coil-coil regions, CC1 and CC2, a leucine zipper, and a c-terminal zinc finger (ZF) (Figure 1.3). Ubiquitin is necessary for complete function of NEMO. The presence of ubiquitin is important for NEMO's role in the activation of IKK2.

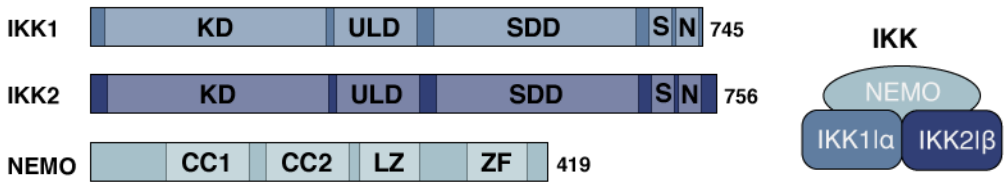

Figure 1.3. Schematic representation of IKK proteins.
This is a schematic representation of IKK proteins showing relevant structural elements. The catalytic subunits, IKK1 and IKK2, have a kinase domain, along with a ubiquitin-like domain, A scaffolding dimerization domain, a serine-rich region, and a NEMO binding domain. NEMO has two coil-coil regions, a leucine zipper, and a zinc finger.

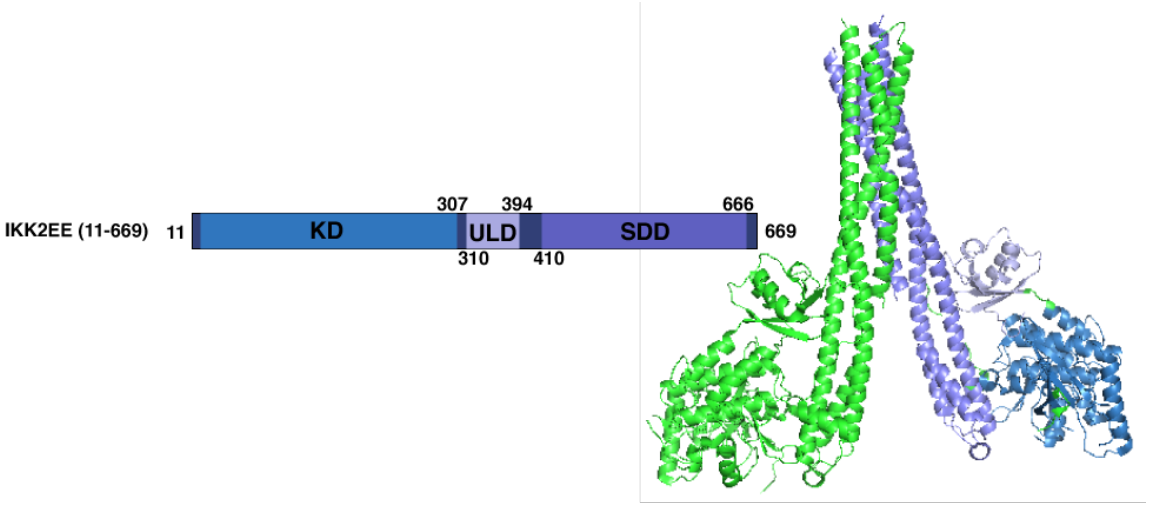

Figure 1.4. Schematic representation of IKK2 along with structure.
This is a schematic representation of IKK2 with the prominent domains color-mapped onto the one monomer of the IKK2 dimer structure. These domains include the KD, the ULD and the SDD.

C. Activation Pathways of NF-κB

There are two activation pathways, the canonical and noncanonical. IKK2 along with NEMO are important for the activation of NF-κB through the canonical pathway. An important part of the signaling cascade is the phosphorylation of IKK2. Though IKK2 is capable of autophosphorylation, several upstream kinases may also be able to phosphorylate IKK2. It is unclear whether any of these upstream kinases are necessary for any specific IKK activation signal. In this canonical pathway, IKK2 phosphorylates n-terminal serines in the IκBs, thus targeting them for ubiquitination and degradation by the 26S proteasome. In the case of IκBα, these serines are residues 32 and 36. The NLS of NF-κB is exposed upon IκB degradation thus freeing the dimer to translocate to the nucleus where it represses or enhances transcription. The p50:RelA heterodimer is the most dominant form of NF-κB activated by the canonical pathway. To some extent RelA:RelA, p50:cRel and cRel:cRel dimers are also activated by this pathway. The amount and time of activation of these dimers depends on the cell type and the stimulus.

In the non-canonical pathway, IKK1 is the necessary kinase for activation of a different form of NF-κB. NIK is known to be a necessary upstream kinase for the phosphorylation of the activation loop serines 176 and 180 of IKK1 and thus for the activation of this alternative pathway. The non-canonical pathway is activated by stimuli such as CD40, LT-beta, and BAFF. Once phosphorylated IKK1 initiates the processing of p100 to p52 which then forms a heterodimer with RelB before translocating to the nucleus.

As the canonical pathway is more responsible for rapid activation of preformed NF-κB, it plays a bigger role in inflammatory diseases where NF-κB activation has gone awry. Therefore, IKK2, the primary culprit for constitutive NF-κB activation, has been the subject of intense study by many groups. Many inhibitors have been developed for IKK2 but few have made it to clinical

trial due to untenable side effects.

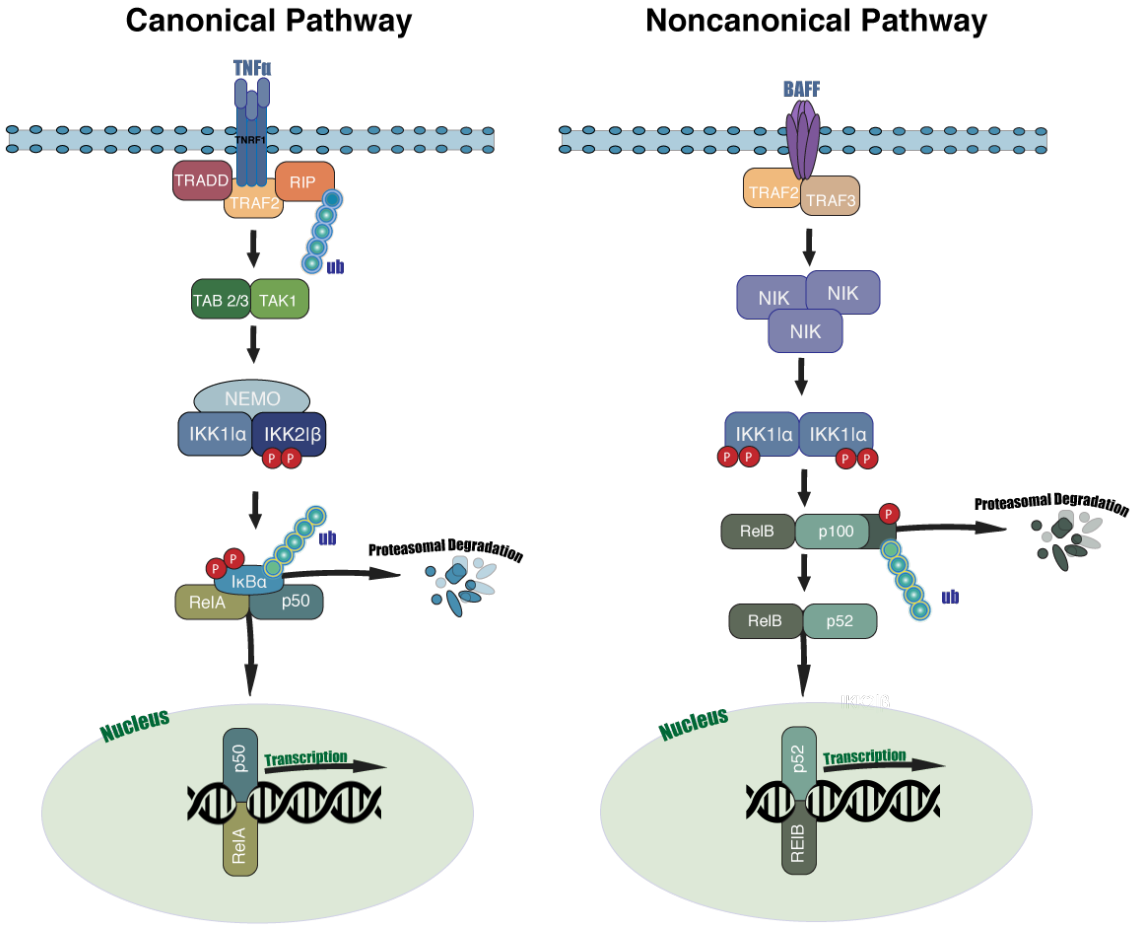

Figure 1.5. Two major NF-κB activation pathways.
The two pathways of NF-κB are the canonical pathway and the non-canonical pathway. Here they are represented by a schematic drawing. IKK2 and NEMO are essential to activating NF-κB in the canonical pathway, while NIK and IKK1 are essential for NF-κB activation in the non-canonical pathway.

D. NF-κB and Disease

Given that NF-κB plays an active role in immune response, cell survival, cell proliferation, creation of new blood cells, and other cell-sustaining mechanisms, its involvement in the genesis and propagation of a number of diseases is unsurprising. Disease states may arise from both hyper- or hypo-activation of the NF-κB pathway. Diseases may also result from mutations in any of the proteins acting along the pathway. Therapeutic strategies for treating NF-κB related diseases have focused on treatments for inflammatory disorders and cancers.

Many cancers and cancer-promoting disease arise from a hyper activation of the NF-κB pathway resulting from a constitutively active NF-κB (Karin, 2006). Although mutations of genes in the NF-kB activation pathway can cause cancers, most frequently cancers are linked to constitutive IKK2 activation. The constitutively active form of NF-κB help prevent death of cancer cells, promote growth and proliferation of cancer cells, and increase the chances of metastasis (Park and Hong, 2016). Some cancers may lead to mutations in proteins important to the NF-κB pathway thereby causing a dysregulation that promotes cancer cell survival. Resulting diseases include non-Hodgkin lymphoma, breast cancer, colorectal cancer, multiple myeloma, and virus-induced Leukemia.

Dysregulated inflammation has been linked with the development of cancer as well as other diseases such as arthritis, sepsis, muscle wasting disease, insulin resistance, and neurodegenerative disorders (Wong and Tergaonkar, 2009). NF-κB activates transcription of genes that produce proinflammatory products, therefore its overactivation can lead to chronic inflammation. Given the wide range of pro-inflammatory molecules regulated by NF-κB through its canonical activation pathway, treatments schemes are often unable to target all sources of pathological inflammation.

Some diseases result from under-activation of NF-κB. *Incontinentia pigmenti* (IP) is a hereditary disease that results when the gene encoding NEMO does not function properly. Survival to birth with this disease is associated with heterozygous females as homozygous cases and male cases do not general result in live birth. The disease results in the production of truncated NEMO that is ineffective in producing activated NF-κB. The disease symptoms include severe skin disorders such as hyperpigmentation, blisters, boils, disorders of the teeth, alopecia, and in a small number of cases, neurological impairment.

E. Inhibitors of IKK2

The IKK complex and specifically the catalytic subunit IKK2 are essential to activation of NF-κB in the canonical pathway. As this pathway activates the most abundant form of NF-κB, the RelA/p65:p50 heterodimer, therapeutic targets focus on its inhibition. Given that aberrant canonical NF-κB behavior has been mostly linked to aberrant activation of IKK2, therapeutic models focus on developing effective inhibitors of IKK2.

There are several classes of IKK2 inhibitors including ATP competitors, allosteric inhibitors, NEMO-binding peptides, and thiol-reactive species (Gilmore and Garbati, 2010). Developed IKK2 inhibitors have been mostly ATP-competitive inhibitors. ATP-competitive inhibitors often lack the level of kinase specificity necessary for effective drug development. This thesis discusses research using cell-based assays, HDX (hydrogen deuterium exchange) and mass spectrometry to analyze the effectiveness and functionality of a number of IKK2 .

ATP competitors have been studied for this thesis mostly for the benefit of obtaining comparative data, while research concentration will be on developing allosteric inhibitors. As IKK is a kinase important to normal cellular function, the more finely tuned inhibition possible with allosteric inhibitors is desirable.

G. Focus of Study

The main focus of our lab is to develop highly specific allosteric inhibitors against IKK2. To accomplish this, both cell-based and *in vitro* experiments are required. In the early phase of this study, our lab identified an allosteric pocket in IKK2. Using virtual screening and follow-up cellular work, one small molecule (compound #65.5) was identified that inhibited IKK2 activation with IC_{50} ~5-10 μM. My goal is to test whether the inhibitor binds to the pocket identified by virtual screening. My plan is to express and purify IKK2 (11-669 EE) from baculovirus infected Sf9 insect cells. I will use purified protein to study both ATP-competitive and allosteric inhibitors. The most critical of *in vitro* assays is the use of HDXMS to determine whether the peptide segments comprising the allosteric pocket are truly the inhibitor binding pocket. Since the compound is a maleimide derivative with potential to make covalent bonds at the cysteines, I wanted to investigate whether the inhibitor is a covalent inhibitor. To test this, my plan is to use MS-MS to identify peptides cross-linked to the inhibitor. Finally, I plan to use crystallography to determine the structure of IKK2 bound the inhibitor. In addition, our collaborator has synthesized two molecules (#65.5.2 and #65.5.3) as probes to confirm whether our inhibitor functions as expected (Figure 3.4). These two molecules are derivatives of compound #65.5 that allow comparison of the effectiveness of different moieties present in #65.5. Compound 65.5.2 is less toxic but less effective, while compound #65.5.3 is more effective but more toxic (Table 1.1 and Figure 3.4).

Table 2.1. The IC_{50} values for the synthesized inhibitors.

Inhibitor	IC_{50} Value
65.5	~5-10 μM
65.5.2	~50-100 μM
65.5.3	~ 1 μM

II. Materials and Methods

A. Baculovirus Expression

1. Sf9 Cell Culturing

Sf9 cells were maintained in culture at 1-3 million cells/mL in Sf9 III medium supplemented with 1% PSG at 170 rpm and 27°C at no more than 1/3 sterile flask volume. Cells were passaged every 24-48 hours.

2. Preparation of Plasmid/Bacmid

Gene for expression of IKK2 (11-669 EE) was cloned into pFastBac HTb plasmid by previous lab members. DNA at a concentration of 1-2ng was transformed into DH10 E. coli competent cells by heat shock. DNA was mixed with DH10 cells and left on ice for 30 minutes. Cells were placed in a 42°C water bath for 45 sec then were incubated on ice for 2 minutes. One mL of SOC medium was added to the cells and the cells were placed on a shaker at 37°C for 5 hours.

Cells were spun down at 3000 rpm for 1 minute. Approximately 900 mL of supernatant was removed. The pellet was resuspended in the remaining media and was plated onto LB agar plates with the following antibiotic concentrations: Kanamycin 50ug/ml, Gentamycin 7ug, Tetracycline 10ug, X-Gal 100ug/ml, and IPTG 40ug/ml.

Plates were placed covered in foil and were left to incubate at 37°C for 48 hours. After 48 hours, 4-6 white colonies and one blue colony were streaked onto a second LB agar plate with antibiotics and placed at 37°C for 48 hours. White colonies were selected and incubated overnight at 37°C in 3mL of SOC media supplemented with Kanamycin 50ug/ml, Gentamycin 7ug/ml and Tetracycline 10ug/ml.

3. Viral Amplification

The P1 viral stocks were created by transfecting Sf9 cells at 0.5 million cells/mL in 2 mL total volume of un-supplemented SF-900 media in 6-well plates. Plates were placed at

27°C for 30 minutes for cells to adhere. To the cells were added 6 µL of Cellfectin (Invitrogen), 1 µg of bacmid DNAs following the Bac-to-Bac Invitrogen protocol. The plate was left to incubate at 27°C for 5 hours after which the media was aspirated and fresh un-supplemented SF-900 media was added. The plate was placed at 27°C for an additional 96 hours at which time the supernatant containing the virus was collected. The supernatant was added at 1:25, 1:50, and 1:100 dilutions to cells plated at 0.5 million cells/mL in 6 well plates. After 72-96 hours of incubation at 27°C, the supernatant was harvested and was kept at 4°C. The cells were washed and lysed with RIPA buffer. Western blot was used to determine the optimum concentration of virus. Using the optimal concentration P3 viral stock was created using 22 million cells in a 15 cm plate infected at the optimal concentration and incubated for 72-96 hours.

4. Large Scale Protein Expression

Sf9 cells were infected at the optimal dilution of virus stock to culture volume as determined during P2. The cells were at a concentration of 1.5-1.75 mil/mL when infected and were left for 48-72 hours at 170 rpm and 27°C. After 72 hours, the cells were collected and spun down at 3000 rpm for 5 minutes. The supernatant was discarded and the cell pellet was kept at -20°C for later purification.

5. Lysis of Sf9 Cells

Cells were lysed in lysis buffer (25mM Tris pH 8.0, 200 mM NaCl, 10 mM Imidazole, 10% Glycerol, 5mM BME, PMSF, mPIC). The cells were lysed by sonication at 5 and 50% duty cycle for two to three 1-minute bursts followed by 5 minutes of rest. The lysate was clarified by centrifugation at 4000 rpm at 4°C for 45 minutes.

B. Protein Purification Protocols

1. Batch Binding Using Nickel Beads

Nickel beads (Ni-NTA resin from Bio Bharati) were equilibrated and then soluble lysate was added to Nickel beads at a 1:1000 dilution. The beads were rotated at 4°C for 4 hours to batch bind. The supernatant was removed and the beads were washed with wash buffer (25mM Tris pH 8.0, 200 mM NaCl, 30 mM Imidazole, 10% Glycerol, and 5mM BME) until the washes checked by Bradford showed a protein concentration of less than 0.1 mg/mL. The protein was eluted in volumes of 1/1000 of the culture size with elution buffer (25mM Tris pH 8.0, 200 mM NaCl, 250 mM Imidazole, 10% Glycerol, and 5mM BME). Between 2-4 fractions were collected and protein concentration was checked using Bradford Assay (Bio-Rad). After running on a SDS-PAGE gel fractions were checked by Coomassie prior to being pooled. Pooled fractions were treated with TEV protease to cleave the His-tag. The protein was incubated with 1mM ATP in 20 mM MgCl2, 20 mM $MgCl_2$, 20 mM β-glycerophosphate, 10 mM NaF, and 1 mM sodium orthovanadate for 1 h and loaded onto a Superose 6 size exclusion column equilibrated with 25 mM Tris-HCl (pH 8.0), 250 mM NaCl, 2 mM DTT, and 5% glycerol.

2. Size-Exclusion Column Chromatography

Purified protein was loaded onto a Superose 6 (GE Healthcare) column in a buffer of 25 mM Tris-HCl pH 8.0, 250 mM NaCl, 5% Glycerol, and 2 mM DTT. Peak fractions were analyzed by loading into a 10% SDS-PAGE and then were pooled, were flash frozen with liquid nitrogen, and were stored at -80°C.

C. *In vivo* Assays

1. IKK2 Inhibitor Assays

Cells (HeLa and 3T3) were plated at a cell count of 150,000 cells per well in 24-well plate

overnight at a total volume 500 μL in DMEM media supplemented with PSG and FBS. Inhibitor was added at various concentrations and incubated for 2 hours (37°C and 5% CO_2). TNFα was added at concentrations between 10 and 20 ng/mL for 15 minutes. Cells were washed and lysed with RIPA Buffer.

D. *In vitro* Assays

1. IKK2 Kinase Assay

The assay was carried out in a buffer (25 mM Tris 7.5, 100 mM NaCl, 10 mM $MgCl_2$, 2 mM DTT) using 50 ng of kinase (IKK2 11-669 EE and IKK2 FL EE), with or without NEMO (50 ng), along with substrate IκBα and both cold and ^{32}P-labeled ATP.

2. IKK2-Inhibitor Kinase Assays

Kinase was incubated in the presence of SC-514 and compound #65.5. Each reaction contained 100 ng IKK2/β kinase and 1 μg of substrate. The reaction was incubated at room temperature for 30 min followed by SDS-PAGE separation and autoradiography.

E. Western Blot

1. Antibodies

IκBα antibody was purchased from Santa Cruz Biotechnology. IKK2, His, and IL-1β antibody and rabbit polyclonal antibodies were purchased from Bio Bharati.

2. Procedure

Cell lysate was loaded onto SDS-PAGE gel and run for 90 minutes at 150V. The separated protein was transferred onto PVDF membrane using wet transfer by running for 90 minutes at 400 mAmp. The membrane was blocked at room temperature for 1 hour with 3% BSA before incubating in primary antibody overnight at 4°C. The membrane was then

incubated with secondary antibody (Bio Bharati) for 1 hour at room temperature. The membrane was developed with 2 mL ECL buffer (0.1 mM Tris 8.6) with addition of 4.4 µL p-coumaric acid, 10 µL luminol, and 1.5 µL H_2O_2).

F. Hydrogen-Deuterium Exchange Mass Spectrometry

Hydrogen-deuterium exchange mass spectrometry (HDXMS) was performed using a Waters Synapt G2Si equipped with a nanoACQUITY UPLC system with HDX technology and a LEAP autosampler. Following purification using nickel beads and size exclusion chromatography, IKK2 (11-669 EE) was incubated with inhibitor for 30 minutes. The protein was at a concentration of 5 µM and the inhibitor at a concentration of 200 µM. For each deuteration time, a portion of sample was equilibrated to 25 °C for 5 min and then mixed with D_2O buffer (25 mM Tris pH 8.0, 200 mM NaCl, 1 mM DTT, 0.5 mM EDTA) for 0, 0.5, 1, 2, or 5 min. The exchange was quenched with an equal volume of quench solution (3 M guanidine, 0.1% formic acid, pH 2.66) at 0°C.

The quenched sample was injected into the 50 µL sample loop, followed by pepsin digestion. The resulting peptides were captured on a BEH C18 Vanguard pre-column, separated by analytical chromatography (Acquity UPLC BEH C18, 1.7 µM, 1.0 X 50 mm, Waters Corporation) using a 7-85% acetonitrile in 0.1% formic acid over 7.5 min, and electro-sprayed into the Waters SYNAPT G2Si quadrupole time-of-flight mass spectrometer. The mass spectrometer was set to collect data in the Mobility, ESI+ mode. The ID runs for IKK2 11-669 EE were conduction with protein at a 10 µM concentration. Peptides were identified using triplicate MSE analyses. The data were analyzed using Waters Corporation software PLGS 2.5. The peptides identified in PLGS were then analyzed in DynamX 3.0 also produced by Waters Corporation.

G. Crystallography

Crystals were obtained using the hanging drop vapor diffusion method as previously described. Protein sample was mixed with inhibitor at a 1:2 molar ratio and incubated for 30 minutes. A 1 µL sample was mixed with 1 µL of reservoir solution containing 1.2 to 2.2 M sodium malonate at pH 5.8, 6.0 and 6.2, 0.3 M ammonium acetate and 10 mM DTT. The 2 µL solution was equilibrated hanging over the reservoir solution at 18°C.

H. Mass Spectroscopy

Protein sample was incubated with inhibitor for 30 minutes with 2 mM DTT to break any disulfide bonds between cysteines that might block interactions with the inhibitors being tested. The sample incubated with inhibitor along with sample incubated without inhibitor was run on an SDS-PAGE gel and stained with Coomassie. The relevant bands were then excised with a razor and submitted for MS analysis.

III. Results

A. IKK2 11-669 EE Expression and Purification

Our lab generated a catalytically active fragment of IKK2 (IKK2 11-669 EE), crystallized the fragment, and determined the x-ray crystal structure of the protein (Polley 2013). Since my goal was to use the same fragment for all my *in vitro* experiments, I will in the future crystallize the active fragment in the presence of inhibitor #65.5 that has recently been identified in our lab. For the present I have focused on optimizing my ability to express and purify IKK2 11-669 EE.

IKK2 expresses well in Sf9 cells using the baculovirus expression system. Previous lab members cloned the gene for expression of IKK2 11-669 EE into pFastBac HTB. I miniprepped this plasmid, and then I transformed the DNA into DH10 E. coli competent cells using heat shock. I isolated the recombinant bacmid using blue/white selection. White colonies contained the DNA of interest and blue colonies lacked this DNA. This bacmid was then used to transfect Sf9 cells thus producing recombinant baculovirus. The virus was amplified, and an optimum dilution was determined before the virus was used for large scale expression.

The his-tagged IKK2 11-669 EE protein was purified using nickel beads while following a batch binding protocol. Between two and three elutions were then pooled together and treated with TEV protease to cleave the poly-histidine fusion tag. Following TEV treatment, the protein was incubated at room temperature with ATP. The cleaved segment was separated using a Superose 6 size exclusion column.

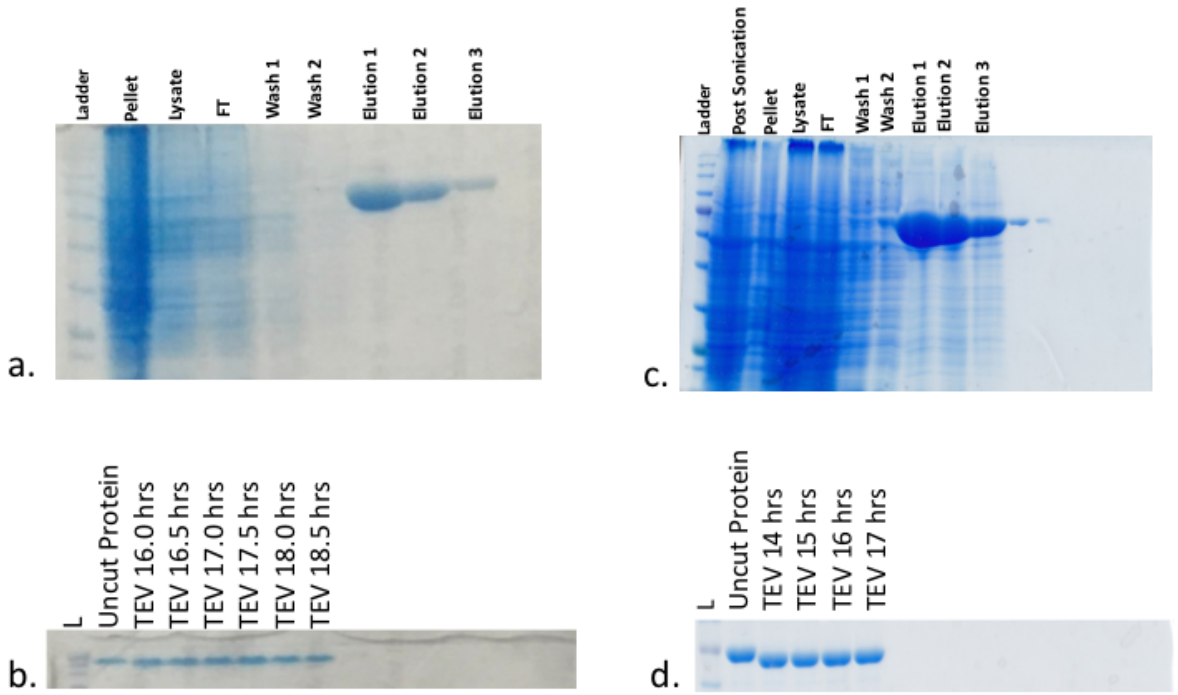

Figure 3.1. Purification of truncated IKK2 11-669 EE.
IKK2 11-669 EE was purified using nickel beads (a) and (c) Two examples of purified IKK2 11-669 EE protein detected by SDS-PAGE using Coomassie stain. The purified protein was treated with TEV protease to cleave the poly-histidine fusion tag. Different timepoints of TEV treatment were loaded onto SDS-Page and detected by Coomassie stain (b) and (d).

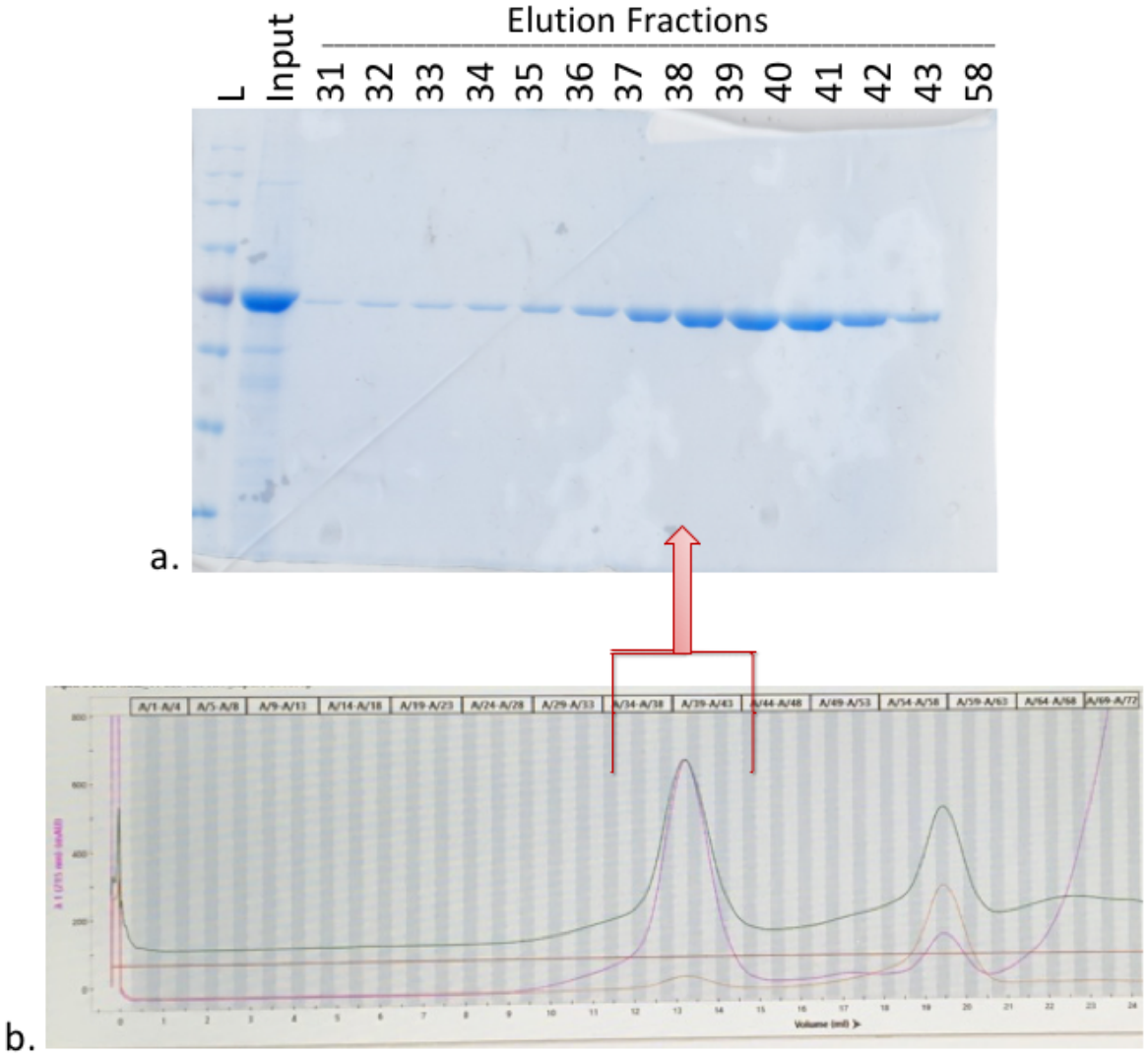

Figure 3.2. Nickel-purified and TEV and ATP-treated IKK2 11-669 EE was loaded onto a Superose 6 size exclusion column. Relevant fractions were pooled, concentrated, then flash frozen with liquid nitrogen in small aliquots.

B. IKK2 11-669 EE is more active *in vitro* than full length IKK2 EE

IKK2 FL EE or IKK2 11-669 EE was incubated with IκBα, cold ATP, and hot ATP containing ^{32}P ATP, both with and without NEMO. The amount of kinase and NEMO used was 50 ng. Aliquots of the experiment mixture were removed from the reaction tube and quenched at different time points (5, 10, and 15 minutes) by adding SDS buffer. Using this assay IKK2 11-669 EE was the more effective kinase toward the IκBα substrate across all time points when compared to the full length protein as evidenced by the greater amount of phosphorylated IκBα in samples containing the truncated kinase (Figure 3.3).

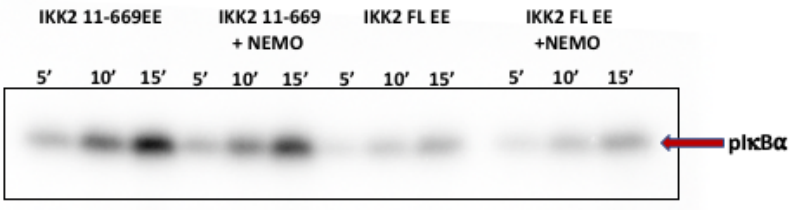

Figure 3.3. *In vitro* kinase assay of IKK2 11-669 EE and IKK2 FL EE with IκBα substrate. IKK2 11-669 (50ng) or IKK2 FL (50ng) along with IκBα, cold ATP, with and without NEMO (50ng) was treated with ^{32}P-labeled ATP for the following time points: 5, 10, and 15 minutes. This experiment was performed working as a team with Myung Ko.

C. #65.5 inhibits IKK activation *in vivo*

I repeated *in vivo* experiments with IKK2 inhibitor #65.5 using a protocol developed by previous lab member Dr. Maria Mulero. Inhibitors #65.5, #65.5.2, and control TPCA1 proved to be effective inhibitors in cell-based assays (Figure 3.4a). The inhibitors were tested in HeLa cells and 3T3 cells. Using titrations that included inhibitor concentrations of 1, 5, 10, 25, 50, and 100 μM, 25 μM was found to be sufficiently inhibitory across the effective inhibitors tested, and therefore this concentration was the default for further inhibitor assays. Western blot using anti-IκBα was used to confirm the amount of IκBα present. Samples with effective inhibition show greater presence of IκBα. Note that inhibitor #65.5 was toxic to cells at 100 μM concentration.

a.

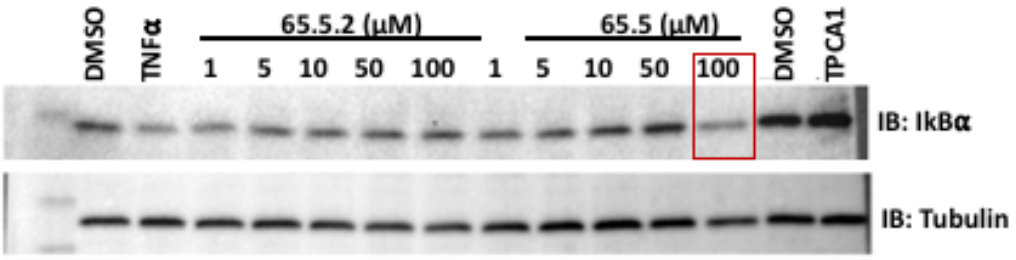

b.

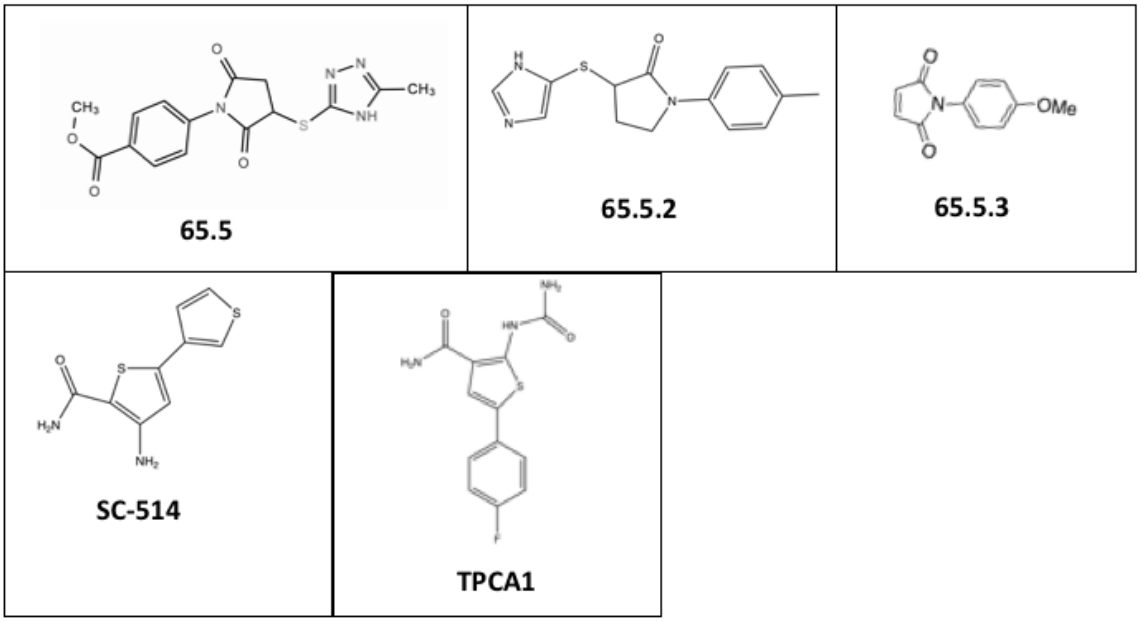

Figure 3.4. ***In vivo*** **assays of inhibitor efficacy by looking at IκBα degradation and inhibitor structures.** In (a) 150,000 3T3 cells/well plated in 24-well plate overnight. Total volume in each well was 500 μL. Inhibitors above were added at μM concentration indicated for 2 hours. TNFα was added at 10 ng/mL for 15 minutes. Note that inhibitor #65.5 is toxic to cells at 100 μM concentration. In (b) the structures of all the inhibitors used are shown.

D. #65.5 does not inhibit catalytic activity of active IKK2

Dr. Gourisankar Ghosh performed a kinase assay to test whether compound #65.5 could inhibit the kinase activity of active IKK2. Since IKK2 11-669 EE is already active, we expected that #65.5 would not be able to inhibit IKK2 catalytic activity as we propose that this compounds works as an allosteric inhibitor. As a control we used SC514, an ATP competitive inhibitor. As expected, SC514 inhibited substrate phosphorylation, but #65.5 did not. These results suggest

that #65.5 functions as an allosteric inhibitor as predicted by our model rather than as an ATP competitor.

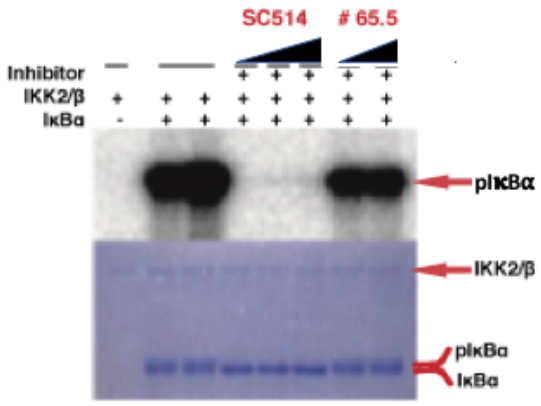

Figure 3.5. *In vitro* kinase assay showing effect of inhibitors on IKK2 EE kinase activity. IKK2 (100 ng)was incubated with IKK2 inhibitors SC514 at three concentration (ATP competitive inhibitor) or #65.5 at two concentration (proposed allosteric inhibitor) along with its substrate IκBα (1 µg) and treated with ^{32}P-labeled ATP. Experiment performed by Dr. Gourisankar Ghosh. This assays shows that SC514 was able to prevent phosphorylation of IκBα while #65.5 was not. The gel was Coomassie stained to show input levels of IKK2 and IκBα.

E. Hydrogen-Deuterium Exchange Mass Spectrometry Data

I tested whether #65.5 binds to a pocket identified in a virtual screen performed by the Amaro Lab at UCSD. I first tested a derivative of #65.5, which we named #65.5.3, an inhibitor with stronger inhibition than #65.5, but higher toxicity (Table 1.1). This molecule has a maleimide core containing strongly electrophilic carbons, and it was expected to covalently cross-link with an exposed cysteine (Figure 3.4b). I performed hydrogen-deuterium exchange mass spectrometry (HDXMS) experiments to confirm this prediction. In addition to #65.5.3, I performed HDXMS experiments of free IKK2 11-669 EE as well as IKK2 11-669 EE incubated with ATP and incubated with TPCA1, an ATP competitive inhibitor of IKK2.

The data were collected using the Synapt G2Si mass spectrometer, and the data were analyzed using Waters DynamX 3.0 software. There was 85.1% coverage of IKK2 (11-669 EE)

in the ID run of the protein. This coverage resulted in analysis including 135 peptides. The HDXMS runs included free-protein as well as protein that was incubated with ATP, with TPCA1, and with our inhibitor #65.5.3. For free IKK2 11-669 EE the concentration used was 10 μM. In assays with binding partners IKK2 11-669 EE was at a concentration of 5 μM and the concentration of the partners varied based on the K_d of those partners. IKK2 11-669 EE was incubated with partners for 30 minutes on ice prior to HDXMS runs.

All experiments were run in triplicate. As pepsin is effective at 2.6 pH and 0°C, the condition used to quench the exchange reaction, this protease is used to digest the protein prior to high-performance liquid chromatography to separate the peptides. Waters software identifies peptides using size, mobility, and retention time on the liquid chromatography column.

Areas of high exchange of hydrogen with deuterium indicate regions of the protein that are solvent exposed. Areas of low exchange indicate more tightly folded regions of the protein with less exposure to solvent. When comparing the data for free protein with that of protein incubated with partners, a decrease of exchange with partners when compared to free protein indicates areas where the partner increased the stability of the protein. This decrease in exchange can also indicate a possible place of binding for the partner. I refer to this decrease in exchange as protecting behavior. When there is an increase in exchange with binding partners compared to the amount of exchange seen with free protein, this indicates possible areas of allostery as that region of the protein has become more dynamic and solvent exposed upon binding of the partner. I refer to this increase in exchange as deprotecting behavior.

1. **Dynamic segments of IKK2 11-669 EE map within the loop and linker regions.**

   HDX data shows areas of high flexibility within the kinase domain, particularly residue 15-40, but also residues 41-61 and 75-95 (Figure 3.8). Residues 125-150, 205-

210, 270-280, and 300-310 are more stable regions in the kinase domain (Figure 3.6). Other areas of high flexibility include residues 360 to 410 located mostly in the ubiquitin like domain but crossing over into the scaffold dimerization domain (SDD) (Figure 3.6). The ULD shows some level of exchange throughout the whole region with no completely closed regions (Figure 3.6). The SDD has the least active flexibility of the three regions with areas of high stability in regions 427-455, 563-570, and 495-657 (Figure 3.6). The stability in residues 563-570 is flanked by the highest areas of instability in the SDD, residues 545-563 and residues 570-590 (Figure 3.6).

In the ULD region there is mostly no difference in uptake with inhibitors or ATP. There may be slight allostery with inhibitors in the residues 360-383 and 360-386 with a comparison of these residues showing that residues 384-386 may be more important to this change (Figure 3.10). The ULD shows flexibility throughout that whole region of the protein (Figure 3.6).

Uptake in the SDD is mostly the same comparing free protein with #65.5.3 bound protein. Areas of allostery when kinase is incubated with compound #65.5 include residues 466-475 and 466-485 with residues 476-485 being more significant to that difference (Figure 3.11). Comparing residues 492 to 503 and 494 to 503, shows that residue 492-493 may be significant to allostery in residue 492-503 (Figure 3.12). Some allostery is also seen in residues 548-562 among others (Figure 3.12).

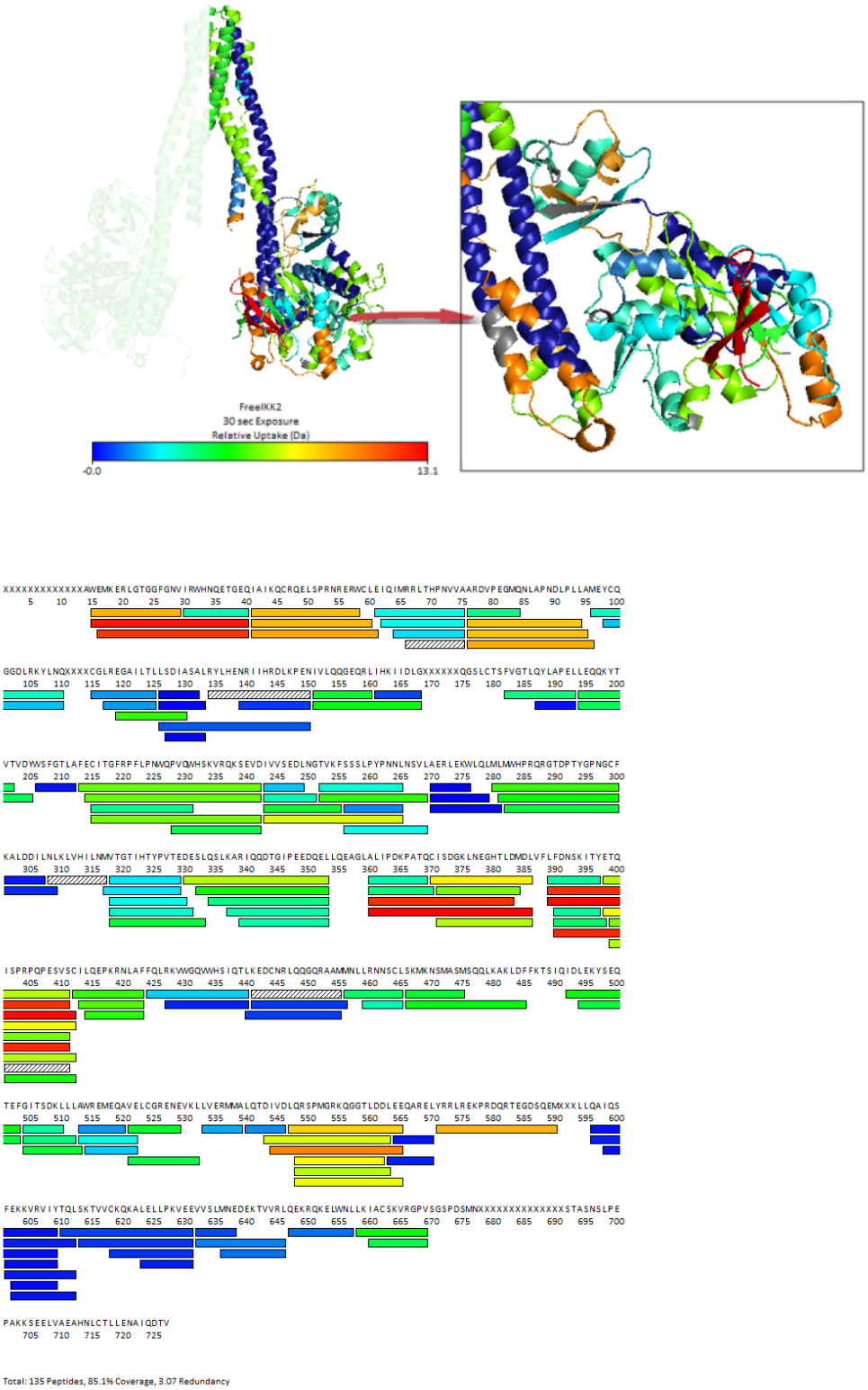

Figure 3.6. Color-coded representation of IKK2 11-669 EE protein dynamics. IKK2 11-669 EE HDX data with relative uptake associated with blue for stable regions and red for dynamic regions.

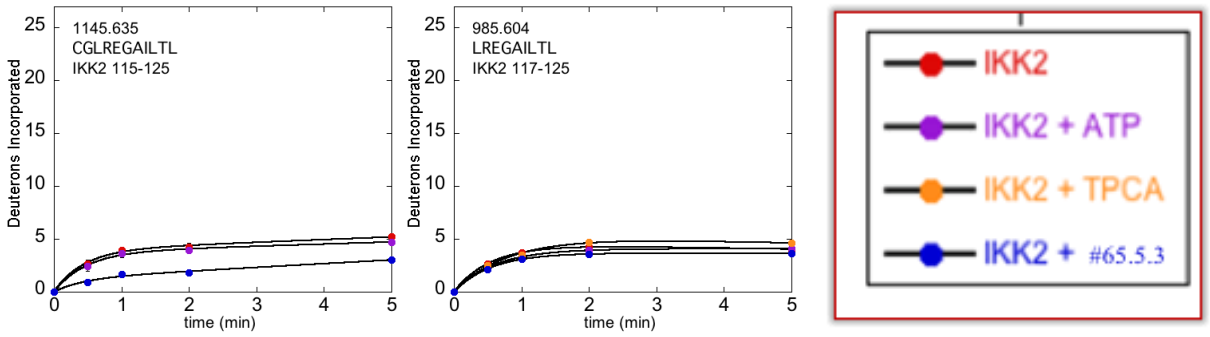

Figure 3.7. HDX residues 115-125 and 117-125 and Legend for HDX.
Inhibitor #65.5.3 shows protection in residue 115-125. Comparing residues 115-125 with 117-125 narrowed the significant residue for this protection and possible binding residue to cysteine 115.

2. Protection of only two peptides is different with #65.5.3 bound

In reviewing this HDX data below red is free IKK2 11-669 EE protein kinase, blue is kinase incubated with #65.5.3, purple is kinase incubated with ATP, and orange is kinase incubated with TPCA1 as shown in the legend (Figure 3.7).

Compound #65.5.3 is a derivative of our proposed allosteric inhibitor #65.5 and shows deprotection throughout all the domains of the protein with two exceptions. With residue 115-125 and possibly residue 117-125 (Figure 3.7), #65.5.3 results in protection. These two residues are the only to show protection when IKK2 11-669 EE is incubated with #65.5.3.

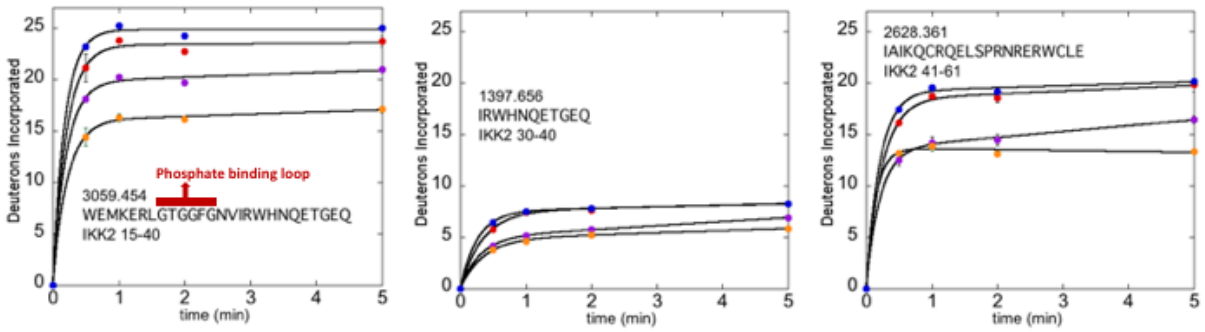

a. **GTGGFG** = Phosphate binding loop
HD Exchange: **TPCA** < **ATP** < **Free IKK2** < **65.5.3**

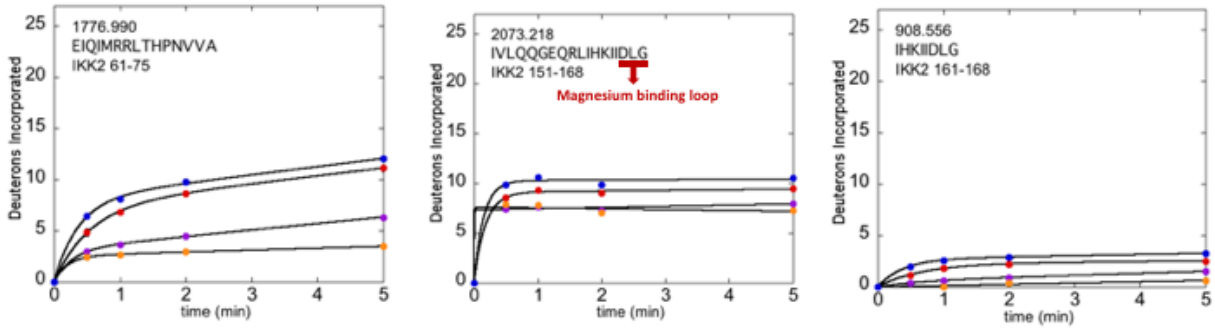

b. **DLG** = Mg^{2+} binding loop
HD Exchange: **TPCA** = **ATP** < **free IKK2** < **65.5.3**

Figure 3.8. Residues 15-40, 30-40, 41-61, 61-75, 151-168, 161-168.
ATP-competitor TPCA1 shows protection as does ATP while #65.5.3 shows deprotection in (a) the ATP-binding loop and (b) the magnesium binding loop as well as surrounding peptides.

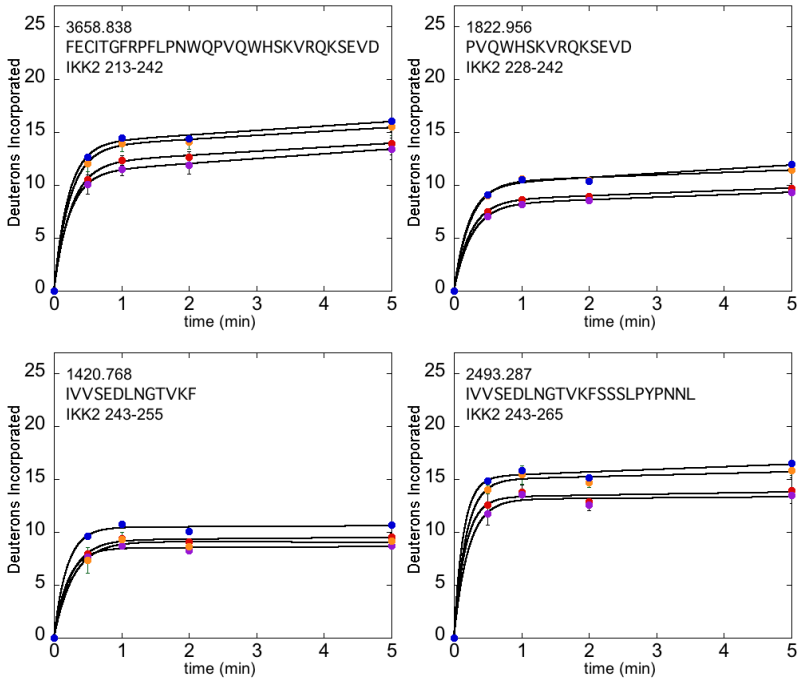

Figure 3.9. Residues 213-242, 243-265, 243-255. Deprotection from inhibitors in the kinase domain with some difference seen in residue 243-255.

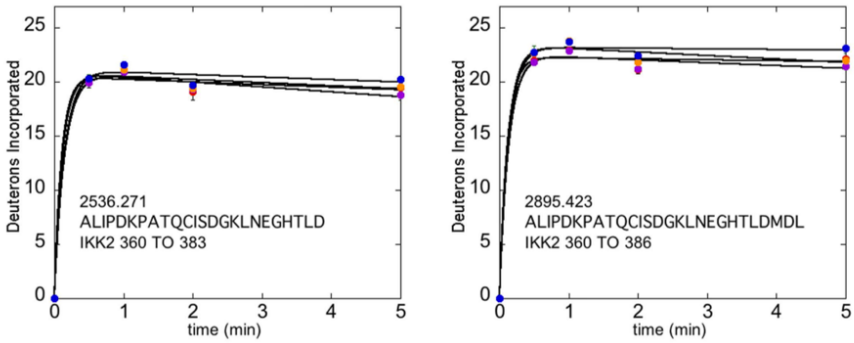

Figure 3.10. HDX residues 360-383 and 360-386. There is flexibility throughout the whole ULD with ATP, TPCA1 and #65.5.3 causing little difference.

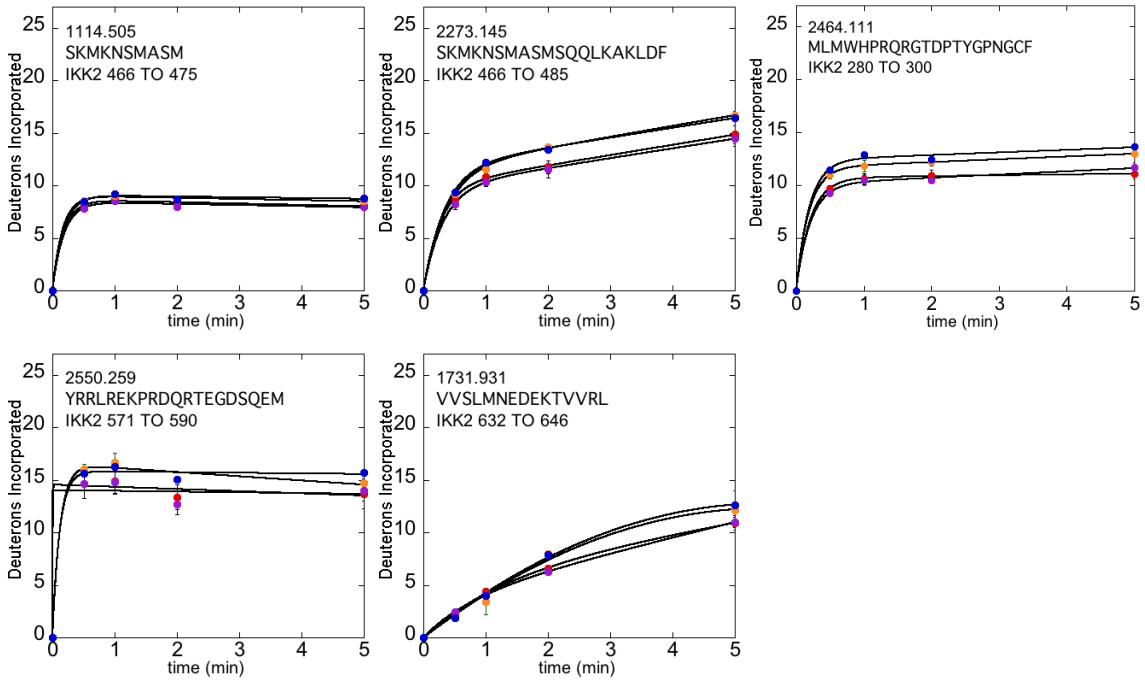

Figure 3.11. HDX residues 466-475 and 466-485, 280-300, 571-590, and 632-646.

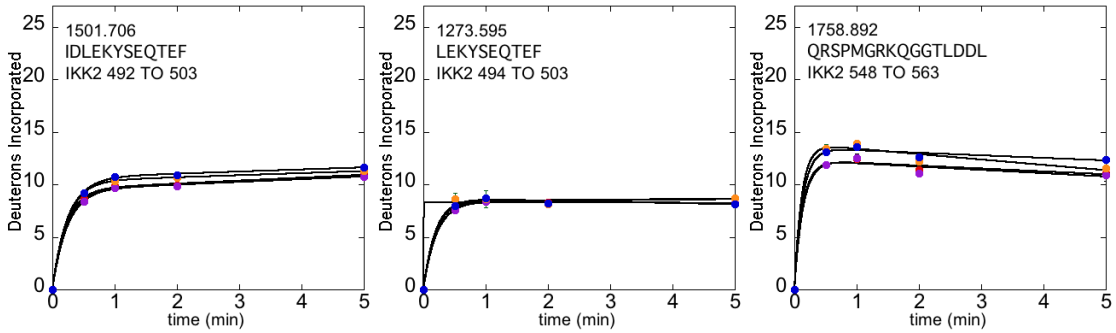

Figure 3.12. HDX residues 492-503 and 494-503, 548-563.

3. TPCA1 and ATP protect distinct but overlapping segments.

TPCA1 is in the class of IKK2 inhibitors that work to prevent effective IKK2 activity by competing with ATP. HDX data confirm that TPCA1 is an ATP competitor as its possible areas of binding overlap with those of ATP for most areas of the protein.

Though further assays such as x-ray crystallography would be necessary to separate areas of inhibitor binding from areas where inhibitor binding leads to increased stability, the data show clear correlation in effect of ATP and TPCA1 as far as areas of reduced exchange along the protein backbone of IKK2 11-669 EE.

When looking at the kinase domain of IKK2 11-669 EE and comparing ATP competitor TPCA1 with proposed allosteric inhibitor #65.5.3, #65.5.3 shows the opposite behavior to that of TPCA1 in much of the kinase domain. The most significant differences within this region are seen within the ATP binding loop (Figure 3.8a) and the magnesium binding loop (Figure 3.8b). While TPCA1 shows obvious competition with ATP, #65.5.3 has a noncompetitive activity with ATP in the ATP binding loop and in the magnesium binding loop. In residues where ATP show protection, #65.5.3 shows allosteric interference. The residues that illustrate this behavior include but are not limited to 61-75, 64-75, 151-168, 161-168 (Figure 3.8). These data support our position that #65.5.3 acts as an allosteric inhibitor.

TPCA1 has areas of protection and deprotection in the kinase domain. ATP shows no areas of deprotection in the kinase domain. For residues 76-95 and 76-96 (Figure 3.13), ATP and TPCA1 show similar protecting behavior. Areas of protection by TPCA1 with no protection or deprotection from ATP include residues 15-29, 96-110, and 98-110 (Figure 3.14). Comparing residues 15-29, and 15-40, the shared region of protection between ATP and TPCA1 can be narrowed to possibly begin at residue 30, not residue 15.

Toward the c-terminal end of the kinase domain, TPCA1 and #65.5.3 both result in deprotection while ATP results in protection or no change as seen in residues 213-242, 228-242, and 243-265 (Figure 3.9). Comparing residue 243-255 where only #65.5.3

shows deprotection with residue 243-265 that shows deprotection with both inhibitors, it becomes more clear that the residue responsible for this similar deprotection behavior is 256-265 (Figure 3.9). This begs the question of whether residue 243-255 is important to the allosteric inhibitor nature of #65.5.3 as its behavior here differs from that of TPCA1.

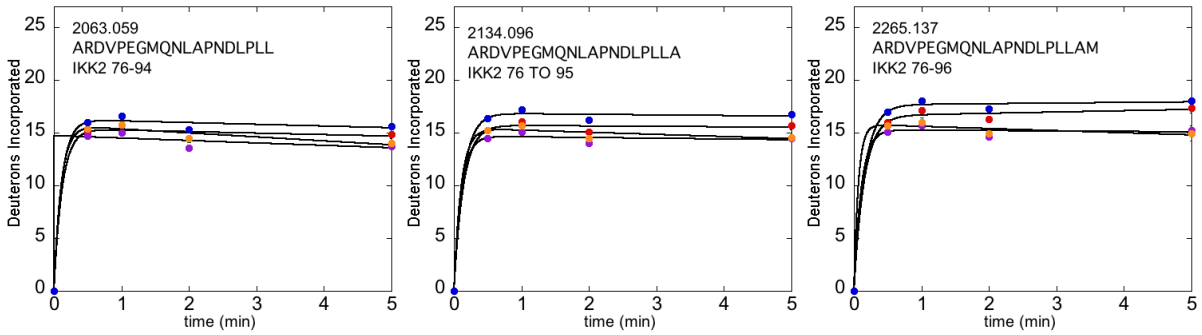

Figure 3.13. HDX residues 76-94, 76-95, 76-96.

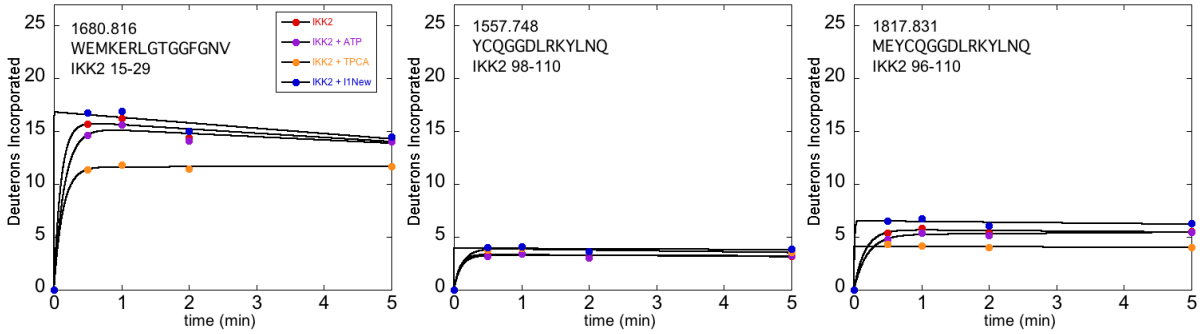

Figure 3.14. HDX residues 15-29, 96-110, and 98-110.

4. Both #65.5 and #65.5.3 covalently cross-linked to IKK2 11-669 EE

MS-MS data showed a mass increase on cysteines 114 and/or 115 when IKK2 11-669 EE was incubated with #65.5 and #65.5.3 in separate experiments (Table 3.1). The mass increases appear to be consistent with reaction products of the inhibitors with

cysteine. Data from two HDX runs, one with DTT and the other without DTT, suggested that there might be binding activity residue 115-125 (Figure 3.7). DTT breaks disulfide bonds, so runs with DTT may have broken disulfide bonds between the neighboring cysteines leaving open the possibility of the inhibitor interacting with these cysteines. Figure 3.15 shows the inhibitor binding pocket (purple) with the two cysteines highlighted in red.

Table 3.1. MS-MS data showing mass changes on cysteines 114 and 115 with inhibitor bound to IKK2 11-669EE.

Mass Change with 65.5		Mass Change with 65.5.3	
K.YLNQFENC{+232.106}CGLR.E	C{+232}	K.YLNQFENC{+438.241}CGLR.E	C{+438}
K.YLNQFENCC{+267.047}GLR.E	C{+267}		
K.YLNQFENCC{+266.046}GLR.E	C{+266}		
K.YLNQFENCC{+242.150}GLR.E	C{+242}		
K.YLNQFENC{+243.135}CGLR.E	C{+243}		
K.YLNQFENCC{+234.073}GLR.E	C{+234}		

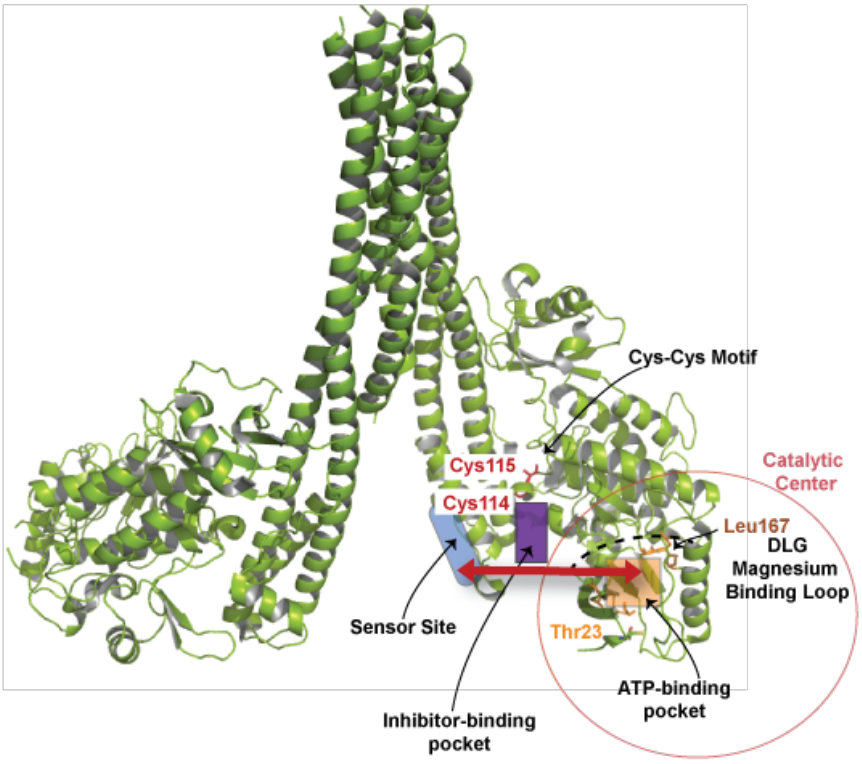

Figure 3.15. The binding pocket for inhibitor #65.5.3. This figure shows the inhibitor binding pocket in purple. Cysteines 114 and 115 are highlighted in red. The magnesium binding loop and ATP binding pocket are both shown. Communication between the sensor site in the SDD and the Catalytic Center necessary for IKK2 activation is disrupted when the inhibitor binds in the pocket.

Acknowledgment

I give special acknowledgment to Myung Ko for her assistance in performing kinase assays with truncated and full-length IKK2 and also again to Professor Ghosh for providing experimental data on kinase function of IKK2 with inhibitors SC514 and #65.5.3.

IV. Discussion

My goal was to determine whether the inhibitors identified through virtual screening are effective and whether they bind to the expected site within IKK2. In order to accomplish this goal I used both cell-based and *in vitro* approaches. I also used HDXMS and MS-MS to confirm possible and real places of binding. Although further studies are needed, the data gained from experiments I have conducted have contributed significantly to accomplishing my initial goals.

Cell-based approaches can use various reporters to determine the efficacy of IKK inhibitors. For example, one can test IκBα degradation in response to a stimulus, RelA nuclear localization, or nuclear NF-kB activity by EMSA. I used IκBα degradation to test inhibitor functionality. IκBα degradation is necessary to expose the nuclear localization signal of NF-kB thus freeing it to translocate to the nucleus. Cell-based assays were conducted in both HeLa cells and 3T3 cells. I found in like manner to previous lab members that #65.5 inhibits IκBα degradation at a concentration of around 10-25 μM (Figure 3.4). It should be noted that #65.5 is toxic to cells at a concentration of 100 μM (Figure 3.4). I conducted assays that showed that inhibitor #65.5.2 is also an effective inhibitor (Figure 3.4). Work performed in our lab by Dr. Maria Mulero also confirmed that #65.5.3 inhibits IκBα degradation at 10-25 μM.

Though cell-based assays were part of my initial investigations, I also conducted *in vitro* experiments. I first purified the IKK2 core fragment (aa 11-669) in its constitutively active state (EE) and found that it is significantly more active kinase than full-length IKK2 (EE). I conducted kinase assays using both the core fragment and the full-length IKK2. These kinases were mixed with IκBα substrate along with cold ATP with and without NEMO added to the mixture. The mixture was then exposed to ^{32}P-labeled ATP for time points of 5, 10, and 15 minutes. Results show that IKK2 11-669 EE was more effective at phosphorylating IκBα (Figure 3.3).

The truncated IKK2 is missing two significant regions. The region encompassing amino acids 670-700 is a serine/proline (SP) rich region. This region has several serines that can be

phosphorylated. This SP region is capable of folding back on itself through inter-domain interactions. These interactions may have a negative effect on substrate binding and or on catalytic activity. The core fragment is also missing the NEMO Binding Domain (NBD). Either of these missing fragments, more probably the SP region, may have an inhibitory effect on the catalytic activity of full-length IKK2. Further kinase assays comparing the IKK2 11-669 EE, IKK2 1-700 EE, and full-length IKK2 EE will clarify this point. In addition HDX studies with inhibitor bound to full-length IKK2 EE will provide data on the dynamics in the SP and NBD both with and without inhibitor bound.

Using HDXMS and MS-MS, a binding site for inhibitor #65.5.3 and #65.5 was located in in the kinase domain within the region predicted. HDXMS data for #65.5.3 showed that cysteine 115 was possibly important to binding of our inhibitor as comparison of two peptides with an amino acid terminus in common allowed the binding activity to be narrowed to this cysteine (Figure 3.7) particularly when combined with MS-MS data. In an effort to substantiate the HDXMD data, MS-MS experiments confirmed a mass change on C115 and/or C114. The program determining the mass change could not reliably distinguish between these two cysteines. Inhibitor #65.5.3 contains particularly electron deficient carbons due to the electron withdrawing effects of carbonyl groups. A covalent bond forms between the nucleophilic sulfur on cysteine and an electrophilic carbon of the inhibitor #65.5.3. The mass increase as shown by MS-MS in the case of #65.5.3 is roughly 438 amu. The mass increase measured with #65.5 varied. Additions to the complex of inhibitor bound to IKK2 such as water and/or derivatives of the inhibitors resulting from hydrolysis reactions may be factors in calculating the masses seen in Table 3.1. More investigation is needed to determine the exact number and form of the inhibitor that binds to the cysteine(s).

Another issue to investigate involves the limited protection seen with #65.5.3 as shown in

HDXMS data. Although the cysteine residue at the point of attachment showed protection in residue 115-127 (figure 3.7), further protection in neighboring residues would be expected as a result of the phenyl moiety in the molecule settling into the attachment pocket (Figure 3.15). Additional protection was not seen in the current data set. Perhaps the phenyl moiety is not completely settling into the pocket, but instead positioned in such a way as to cause allosteric effects.

Binding at C114 and C115 (cys-cys motif) is significant for structural-functional reasons. Binding of #65.5.3 causes conformational changes within the catalytic center of IKK2 11-669 EE. This catalytic center consists of the catalytic loop, the phosphate binding loop, and the magnesium binding loop (MBD) (Figure 3.15). Residues 151-168 and 161-168 (Figure 3.8) which coincide with the phosphate bind loop and the MBD show allosteric effects upon binding of #65.5.3. These same residues, as would be expected, show protecting behavior when bound by ATP or ATP-competitive inhibitor TPCA1. Furthermore, the cys-cys motif is located opposite an IKK2 sensor site located in the SDD that is significant for IKK2 function. Past research in this lab showed that mutation in this SDD sensor region reduced catalytic activity of IKK2 toward IκBα (Polley 2013) (Figure 3.15). The fact that inhibitor #65.5.3 binds to this cys-cys motif that is optimally located to disrupt communication between the catalytic center and the sensor site further supports its function as an allosteric inhibitor (Figures 3.15 and 3.16).

HDX studies confirm that TPCA1 works as an ATP competitor. In the kinase domain it has protecting behavior in residues 15-40, 16-40, 30-40, 41-58, 41-60, 41-61, 61-75, 62-75, and 64-75, 76-94, 76-95, and 76-96, the same as ATP (Figures 3.8 and 3.12). The competitive protection is not complete throughout the kinase domain of IKK2. Areas of protection by TPCA1 with little protection from ATP include residues 15-29, 96-110, and 98-110 (Figure 3.14). TPCA1 shows deprotection in a few areas where ATP shows protection, residues 213-242 and others inside the

kinase domain, but outside the ATP binding pocket (Figure 3.9).

Deprotection for residue 213-242 occurs with both TPCA1 and #65.5.3. Both inhibitors also show deprotection in residues 280-300 while there is no difference in deuterium uptake seen with ATP. In the free protein, peptide 280-300 is a dynamic area flanked on both ends by areas of high stability (Figures 3.6 and 3.8). This area then becomes more dynamic when IKK2 11-669 EE is bound to inhibitors. Other areas of deprotection with TPCA1 and no difference in uptake with ATP include residues 466-485, 571-590, and 632-646 in the SDD (3.11).

The places of allosteric behavior difference between TPCA1 and #65.5.3 may be key areas to focus on for understanding the conformational changes most important for effective allosteric inhibition. As shown by HDX data, these areas include peptides in the kinase domain where #65.5.3 shows deprotection where both ATP and TPCA1 show protection such as in the ATP binding pocket and the magnesium binding domain. The only residue where #65.5.3 shows protection is also the only residue where TPCA1 shows allosteric interference that does not overlap with allostery from #65.5.3. This is best seen viewing residues 117-125 (Figure 3.7). There was no data for TPCA1 for residue 115 to 125 that more clearly shows the #65.5.3 protection.

While effective in blocking the pathway, ATP analogs allow for less fine tuning than allosteric inhibitors. Inhibitors that work through allosteric interference can be more finely tuned in that a conformation that renders the kinase inactive for one substrate my leave the kinase functional for other substrates. IKK is a necessary kinase for the healthy function of normal cells. Fine-tuned inhibition is essential for the development of inhibitors with minimal side effects.

The data I presented in this thesis confirmed that our inhibitors work to block NF-κB using cell-based assays. Both kinase assays and HDXMS data helped confirm that our inhibitors work allosterically. Additionally, HDXMS and MS-MS data established that our inhibitors bind in the predicted binding pocket. Pooling these results we developed a model of how our inhibitors work

(Figure 3.16). These inhibitors bind to the cys-cys motif in a way that disrupts communication between the catalytic domain and the sensor region in the SDD of IKK2. This disruption serves to block or reduce activation of IKK2. Additional HDX studies will be performed using IKK2 FL, and a kinase dead construct of IKK2 to gain further insight.

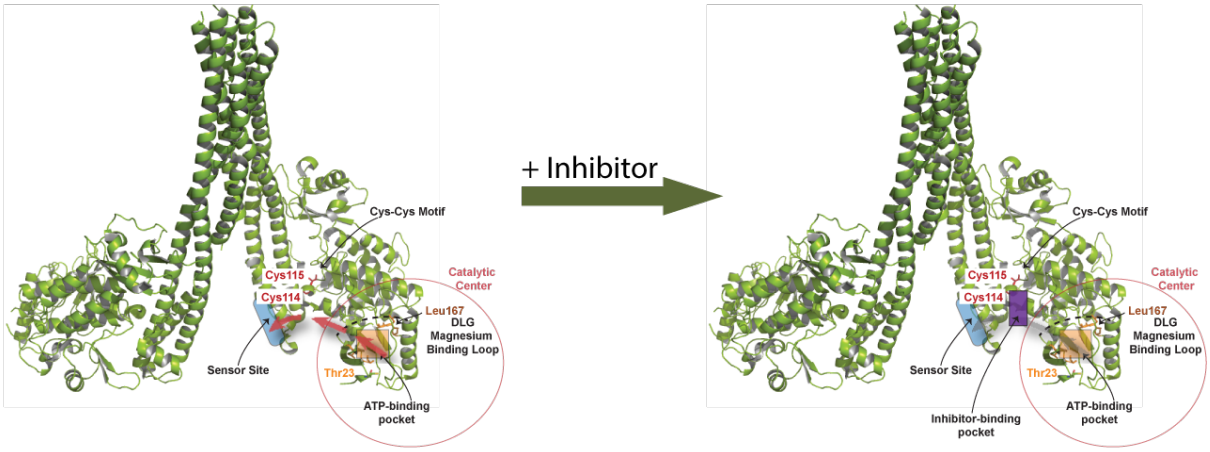

Figure 3.16. Our model of how inhibitor #65.5.3 works. There is communication between the catalytic center and sensor site in the SDD of IKK2 important to its activation. Our allosteric inhibitor binds in the pocket shown in purple thus blocking communication between the catalytic domain and the sensor site preventing activation of IKK2.

REFERENCES

Almaden, J. V., Tsui, R., Liu, Y. C., Birnbaum, H., Shokhirev, M. N., Ngo, K. A., Davis-Turak, J.C., Otero, D., Basak, S., Rickert, R.C. and Hoffmann, A. (2014) A Pathway Switch Directs BAFF Signaling to Distinct NF-κB Transcription Factors in Maturing and Proliferating B Cells. *Cell Reports*, *9*(6), 2098–2111.

Anand, G. S., Hughes, C. A., Jones, J. M., Taylor, S. S., and Komives, E. A. (2002) Amide H/2H Exchange Reveals CommunicationBetween the cAMP and Catalytic Subunit-bindingSites in the RIa Subunit of Protein Kinase A, *Journal of Molecular Biology,* 323, 377-386

Baeuerle, P.A. and Baltimore, D. (1996) NF-κB: ten years after. *Cell*, 87, 13-20.

Baeuerle, P.A. and Henkel, T. (1994) Function and activation of NF-κB in the immune system. *Annual Review of Immunology*, 12, 141-179.

Baldwin, A.S., Jr. (1996) The NF-κB and IκB proteins: new discoveries and insights *Annual Review of Immunology*, 14, 649-683.

Baltimore, D. (2009). Discovering NF-κB. *Cold Spring Harbor Perspectives in Biology*, 1(1), a000026. http://doi.org/10.1101/cshperspect.a000026

Bingham, A. H., Davenport, R. J., Gowers, L., Knight, R. L., Lowe, C., Owen, D. A., … Pitt, W. R., (2004) A novel series of potent and selective IKK2 inhibitors, *Bioorganic & Medicinal Chemistry Letters*, 14(2), 409-412.

Chen, F.E., Huang, D.B., Chen, Y.Q. and Ghosh, G. (1998a) Crystal structure of p50/p65 heterodimer of transcription factor NF-κB bound to DNA. *Nature*, 391, 410-413.

Chen, Y.Q., Ghosh, S. and Ghosh, G. (1998b) A novel DNA recognition mode by the NF-κB p65 homodimer. *Nature Structural & Molecular Biology*, 5, 67-73.

Chen, Y.Q., Sengchanthalangsy, L.L., Hackett, A. and Ghosh, G. (2000) NF-κB p65 (RelA) homodimer uses distinct mechanisms to recognize DNA targets. *Structure*, 8, 419-428.

Chen, Z .J., Parent L., Maniatis, T., (1996) Site-Specific Phosphorylation of IκBα by a Novel Ubiquitination-Dependent Protein Kinase Activity, *Cell*, 84(6), 853-862.

Courtois, G. and Gilmore, T. D., (2006) Mutations in the NF-jB signaling pathway: implications for human disease. *Oncogene*, 25, 6831-6843.

Croy, C. H., Koeppe, J. R., Bergqvist, S., and Komives, E. A. (2004) Allosteric Changes in Solvent Accessibility Observed in Thrombin upon Active Site Occupation, *Biochemistry*, 43, 5246-5255.

Delhase, M., Hayakawa, M., Chen, Y. and Karin M. (1999) Positive and negative regulation of IκB kinase activity through IKKβ subunit phosphorylation. *Science*, 284, 309-313.

Gadina, M., Gazaniga, N., Vian, L., and Y. Furumoto, (2017) Small molecules to the rescue: Inhibition of cytokine signaling in immune-mediated diseases. Journal of Autoimmunity, 85, 20-31.

Gilmore T.D., Garbati M.R. (2010) Inhibition of NF-κB Signaling as a Strategy in Disease Therapy. In: Karin M. (eds) NF-kB in Health and Disease. Current Topics in Microbiology and Immunology, vol 349. Springer, Berlin, Heidelberg.

Greten, F. R., Arkan, M. C., Bollrath, J., Hsu, L., Goode, J.,Miething, C., Göktuna S. I., Neuenhahn, M., Fierer, J., Paxian, S., Van Rooijen, N., Xu, Y., O'Cain, T., Jaffee, B. B., Busch D. H., Duyster, J., Schmid, R.M., Eckmann, L., Karin, M. (2007), NF-κB is a negative regulator of IL-1β secretion as revealed by genetic and pharmacological inhibition of IKKβ. *Cell.* 130(5), 918-931.

Sala E., Guasch, L., Iwaszkiewicz, J., Mulero, M., Salvadó M. J., Pinent, M., Pinent, M., Zoete, V., Grosdidier, A., Garcia-Vallvé, S., Michielin, O., Pujadas, (2011) Identification of Human IKK-2 Inhibitors of Natural Origin (Part I): Modeling of the IKK-2 Kinase Domain, Virtual Screening and Activity Assays. PLoS ONE 6(2): e16903. https://doi.org/10.1371/journal.pone.0016903

Fusco, A.J., Savinova, O.V., Talwar, R., Kearns, J.D., Hoffmann, A. and Ghosh G. (2008) Stabilization of RelB requires multidomain interactions with p100/p52. *Journal of Biological Chemistry*, 283, 12324-12332.

Fusco, A.J., Mazumder, A., Wang, V.Y., Tao, Z., Ware, C. and Ghosh, G. (2016) The NF-κB subunit RelB controls p100 processing by competing with the kinases NIK and IKK1 for binding to p100. *Science Signaling*, 9, 447, ra96.

Ghosh, G., van Duyne, G., Ghosh, S. and Sigler, P.B. (1995) Structure of NF-κB p50 homodimer bound to a κB site. *Nature*, 373, 303-310.

Ghosh, S., May, M.J. and Kopp, E.B. (1998) NF-κB and Rel proteins: evolutionarily conserved mediators of immune responses. *Annual Review of Immunology*, 16, 225-260.

Ghosh, S. and Baltimore, D. (1990) Activation in vitro of NF-κB by phosphorylation of its inhibitor IκB. *Nature*, 344, 678-682.

Ghosh, S. and Karin, M. (2002) Missing pieces in the NF-κB puzzle. *Cell*, 109 Supplement 1, S81-96.

Hayden M.S. and Ghosh, S. (2004) Signaling to NF-κB. *Genes and Development*, 18, 2195-2224.

Hoffmann, A., Natoli, G. and Ghosh, G. (2006) Transcriptional regulation via the NF-κB signaling module. *Oncogene*, 25(51), 6706-6716.

Huxford, T., Huang, D.B., Malek, S. and Ghosh, G. (1998) The crystal structure of the IκB/NF-κB complex reveals mechanisms of NF-κB inactivation. *Cell*, 95, 759–770.

Israël, A. (2010). The IKK Complex, a Central Regulator of NF-κB Activation. Cold Spring Harbor Perspectives in Biology, 2(3), a000158. http://doi.org/10.1101/cshperspect.a000158

Jeon, Y. J., Han, S. H., Lee, Y. W., Lee, M., Yang, K. H., and Kim, H. M. (2000) Dexamethasone inhibits IL-1β gene expression in LPS-stimulated RAW 264.7 cells by blocking NF-κB/Rel and AP-1 activation, *Immunopharmacology*, 48(2), 173-183.

Karin, M. and Ben-Neriah, Y. (2000) Phosphorylation meets ubiquitination: the control of NF-κB activity. *Annual Review of Immunology*, 18, 621-663.

Lennikov, A., Mirabelli, P., Mukwaya, A., Schaupper, M., Thangavelu, M., Lachota, M., Ali, Z., Jensen, L., and Lagali, N. (2018) Selective IKK2 inhibitor IMD0354 disrupts NF-κB signaling to suppress corneal inflammation and angiogenesis, *Angiogenesis*, 21(2), 267-285.

Lu, T., Yang, M., Huang, D.-B., Wei, H., Ozer, G. H., Ghosh, G. and Stark, G. R. (2013) Role of lysine methylation of NF-κB in differential gene regulation. Proceedings of the National Academy of Sciences of the United States of America, 110(33), 13510–13515.

Mandell, J. G., Falick, A. M., and Komives, E. A. (1998) Measurement of Amide Hydrogen Exchange by MALDI-TOF Mass Spectrometry. *Analytical Chemistry, 70(19), 3987-3995.*

Oeckinghaus, A. and Ghosh, S. (2009) The NF-κB family of transcription factors and its regulation. *Cold Spring Harbor Perspectives in Biology*, 1(4), a000034.

Oeckinghaus, A., Hayden, M.S. and Ghosh, S. (2011) Crosstalk in NF-κB signaling pathways. *Nature Immunology,* 12, 695–708.

Polley, S., Huang, D. B., Hauenstein, A. V., Fusco A. J., Zhong, X., Vu, D., Schrofelbauer, B., Kim, Y., Hoffmann, A., Verma I. M., Ghosh, G., Huxford, T. (2013) A Structural Basis for IκB Kinase 2 Activation Via Oligomerization-Dependent Trans Auto-Phosphorylation. *PLoS Biology,* 11(6): e1001581.

Ramirez-Sarmiento, C. A., and Komives, E. A. (2018) Hydrogen-deuterium exchange mass spectrometry reveals folding and allostery in protein-protein interactions. *Methods,* 144, 43-52.

Sharif, O., Bolshakov, V. N., Raines, S., Newham, P., & Perkins, N. D. (2007). Transcriptional profiling of the LPS induced NF-κB response in macrophages. BMC Immunology, 8, 1. http://doi.org/10.1186/1471-2172-8-1

Scheibel, M., Klein, B., Merkle, H., Schulz, M., Fritsch, R., Greten, F. R., Arkan, M. C., Schneider, G., and Schmid, R. M. (2010) IκBα is an essential co-activator for LPS-

induced IL-1β transcription in vivo. The Journal of Experimental Medicine, 207, 2621-2630.

Sen, R. and Baltimore, D. (1986) Multiple nuclear factors interact with the immunoglobulin enhancer sequences. *Cell*, 46, 705-716.

Tak, P. P., & Firestein, G. S. (2001). NF-κB: a key role in inflammatory diseases. *Journal of Clinical Investigation*, 107(1), 7–11.

Tian, F., Zhou, P., Kang, W., Luo, L., Fan, X., Yan, J. and Liang, H. (2014) The small-molecule inhibitor selectivity between IKKα and IKKβ kinases in NF-κB signaling pathway. *Journal of Receptors and Signal Transduction, 35(4), 307-318.*

Truhlar, S. M. E., Mathes, E., Cervantes, C. F., Ghosh, G., and Komives, E. A. (2008) Pre-folding IκBα Alters Control of NF-κB Signaling*, Journal of Molecular Biology*, 380(1), 67-82.

Malek, S., Huang, D.B., Huxford, T., Ghosh, S. and Ghosh, G. (2003) X-ray crystal structure of an IκBβ:NF-κB p65 homodimer complex. *Journal of Biological Chemistry*, 278, 23094-23100.

Pahl, H.L. (1999) Activators and target genes of Rel/NF-κB transcription factors. *Oncogene*, 18, 6853-6866.

Vallabhapurapu, S. and Karin, M. (2009) Regulation and function of NF-κB transcription factors in the immune system. *Annual Review of Immunology*, 27, 693–733.

Wei, H., Wang, B., Miyagi, M., She, Y., Gopalan, B., Huang, D.B., Ghosh, G., Stark, G.R. and Lu, T. (2013). PRMT5 dimethylates R30 of the p65 subunit to activate NF-κB. *Proceedings of the National Academy of Sciences of the United States of America*, *110*(33), 13516–13521.

Weis, D. D. (2016). *Hydrogen Exchange Mass Spectrometry of Proteins*. Wiley.

Wong, E. T., Tergaonkar, V., (2009) Roles of NF-κB in health and disease: mechanisms and therapeutic potential*, Clinical Science,* 116(6), 451-465.

Xia, Y., Shen, S. and Verma, I.M. (2014) NF-κB, an active player in human cancers. *Cancer Immunology Research.* 2(9), 823–830.

Xiao, G., Harhaj, E.W. and Sun, S.C. (2001) NF-κB-inducing kinase regulates the processing of NF-κB2 p100. *Molecular Cell*, 7(2), 401-409.